Technical Report

TR-13-11

Thermodynamic evaluation of Cu-H-O-S-P system

Phase stabilities and solubilities for OFP-copper

Hans Magnusson, Karin Frisk
Swerea KIMAB AB

April 2013

Svensk Kärnbränslehantering AB
Swedish Nuclear Fuel
and Waste Management Co

Box 250, SE-101 24 Stockholm
Phone +46 8 459 84 00

ISSN 1404-0344
SKB TR-13-11
ID 1393418

Thermodynamic evaluation of Cu-H-O-S-P system

Phase stabilities and solubilities for OFP-copper

Hans Magnusson, Karin Frisk
Swerea KIMAB AB

April 2013

Abstract

A thermodynamic evaluation for Cu-H-O-S-P has been made, with special focus on the phase stabilities and solubilities for OFP-copper. All binary systems including copper have been reviewed. Gaseous species and stoichiometric crystalline phases have been included for higher systems.

Sulphur in OFP-copper will be found in sulphides. The sulphide can take different morphologies but constant stoichiometry Cu_2S. The solubility of sulphur in FCC-copper reaches ppm levels already at 550°C and decreases with lower temperature. No phosphorus-sulphide will be stable, although the copper sulphide can be replaced by copper sulphates at high partial pressure oxygen like in the oxide scale.

Phosphorus has a high affinity to oxygen, and phosphorus oxide P_4O_{10} and copper phosphates ($Cu_2P_2O_7$ and $Cu_3(PO_4)_2$) are all more stable than copper oxide Cu_2O. With hydrogen present at atmospheric pressure, copper phosphates $Cu_2P_2O_7$ and $Cu_3(P_2O_6OH)_2$ are both more stable than water vapour or aqueous water at temperatures below 400°C. At high pressure conditions, the copper phosphates can be reduced giving water. However, the phosphates are still more stable than water vapour. The solubility limit of phosphorus in FCC-copper at 25°C is 510 ppm, in equilibrium with copper phosphide Cu_3P. The major part of phosphorus in OFP-copper will be in solid solution.

Oxygen in FCC-copper has a very low solubility. In the presence of a strong oxide forming element such as phosphorus in OFP-copper, the solubility decreases even more. Copper oxides will become stable first when all phosphorus has been consumed, which takes place at twice the phosphorus content, calculated in weight.

Hydrogen has a low solubility in copper, calculated as 0.1 ppm at 675°C. No crystalline hydrogen phase has been found stable at atmospheric pressures and above 400°C. At lower temperatures the hydrogen containing phosphate $Cu_3(P_2O_6OH)_2$ can become stable. Measured hydrogen contents for OFP-copper are higher than the calculated solubility of hydrogen. Experiments and calculations indicate that hydrogen degassing should occur even in hydrogen gas. The strong interaction between oxygen and hydrogen could motivate why hydrogen is trapped in the material at low temperatures in an oxygen containing environment.

Contents

1 Introduction

Oxygen-free phosphorus copper (OFP-copper) is chosen as canister material for spent nuclear fuel. The canister shall prevent the release of radioactive substances to the surroundings, shield radioactivity and prevent criticality (SKB 2010). The canister's barrier and its structural integrity require the OFP-copper to have sufficiently good material properties, such as creep ductility and resistance to corrosion.

The design premises on the copper canisters regarding its compositional limits are based on the experiences of how ppm levels of hydrogen, oxygen, sulphur and phosphorus influence the mechanical and corrosive behaviour (SKB 2009). To obtain the required creep ductility sufficient amounts of phosphorus should be present in solid solution allowing for solution strengthening during creep. The sulphur content should be minimised based on traditional experience how sulphides influence the ductility. Hydrogen is specified to be lower than 0.6 ppm to avoid hydrogen embrittlement during manufacturing (SKB 2009). Oxygen content should be minimised in order to avoid grain boundary corrosion. The element limits are given as phosphorus 30–100 ppm, sulphur less than 12 ppm, hydrogen less than 0.6 ppm, and oxygen less than some tens of ppm (ppm in this report is given as a mass-fraction, if not otherwise stated such as atomic ppm). The requirements on the copper ingots in the initial state are even lower in oxygen, below 5 ppm (SKB 2010).

Thermodynamic calculations can be used to determine the most stable set of crystalline phases, liquids, or gases in equilibrium for a given temperature, pressure, and composition. They can also be used to calculate metastable phases and compare the relative stabilities and possible significance of phases at defined conditions. The solubility of elements such as hydrogen, oxygen, sulphur and phosphorus in copper can be calculated. Thermodynamic modelling offers a valuable tool to couple the influence of trace elements or alloying elements to microstructure, as well as determining the response of a material exposed to an atmosphere or environment. The thermodynamic equilibrium is per definition the most stable state, and consequently offers valuable information on the long-term stability of the material.

The accuracy of the calculations depends on the thermodynamic description of the alloying system that is being used. The CALPHAD approach allows for a critical assessment of alloy systems based on experimental phase diagram and thermochemical information (Lukas et al. 2007). Equilibrium calculations can be made for multi-component systems based on critical assessments of lower ordered systems. Thermodynamic information of pure elements (unary), interaction of two elements (binary), and higher-order systems, are all brought together into a thermodynamic database suitable for multi-component calculations.

The present work is a thermodynamic evaluation of the Cu-H-O-S-P system, allowing for multi-component calculations on phase stability and solubility of hydrogen, oxygen, sulphur and phosphorus in copper. The focus is on low-temperature equilibria, although it is important to evaluate equilibria at higher temperatures as well. For instance, sulphides and oxides can precipitate at high temperature during processing and remain to low-temperature service. Calculations for OFP-Cu have a typical composition of 50 ppm phosphorus, 6 ppm sulphur, 3 ppm oxygen and 0.35 ppm hydrogen (Andersson et al. 2004, SKB 2006, 2010).

A limitation in the present work is that the liquid metal is not modelled in detail. Metal-sulphur and metal-oxygen melts are well known to exhibit strong compositional ordering. However, the calculations should give accurate results for the low concentrations of hydrogen, oxygen, sulphur and phosphorus that are used in this work.

2 Thermodynamic models

2.1 Solution phases and stoichiometric compounds

The state of the system can be defined by its Gibbs energy, a characteristic measure of the free energy for a defined temperature, pressure and composition. By minimising Gibbs energy, the set of phases with their compositions giving a global minimum in energy will define the equilibrium state.

Solution phases in this work are gas, liquid and face-centered cubic (denoted FCC or FCC_A1 in text, where A1 is the crystal designation, *strukturbericht*). These phases are described with different thermodynamic models to describe their properties in the compositional range. These models are commonly used in thermodynamic assessments of many different alloy systems (Saunders and Miodownik 1998, Lukas et al. 2007). The phases are summarised in Table 2-1, with formula or constituents given as well. These models will be briefly reviewed in this chapter. All thermodynamic parameters are given in the Appendix. The thermodynamic calculations in this work will be made using Thermo-Calc software (Thermo-Calc 2010).

The temperature stability of pure elements, stoichiometric compounds, and end-members of solution phases are described with a temperature polynomial. This expression must allow for representing the different types of thermochemical information, such as heat capacity, enthalpy etc. The molar Gibbs energy is of the form:

$$^{o}G_i - \sum_i b_i H_i^{SER} = a + bT + cTlnT + dT^2 + eT^{-1} + \ldots \quad (2\text{-}1)$$

The term $\Sigma_i b_i H_i^{SER}$ represents the sum of the enthalpies of the elements in their reference phases, which are the stable phases at 298.15 K and 100 kPa, except for phosphorus where the white phase is used instead of the stable red phase. The Gibbs energy expressions of pure elements in different phases follow the recommended values according to SGTE, Scientific Group Thermodata Europe (Dinsdale 1991).

The gas phase is described by an ideal substitutional model, and the molar Gibbs energy becomes:

$$G_m^{gas} = \sum y_i \, {}^{o}G_i + RT(\sum y_i ln\, y_i) + RTln\left(\frac{P}{P_0}\right) \quad (2\text{-}2)$$

where y_i is the site fraction of constituent i, $^{O}G_i$ the Gibbs energy of individual constituents, i the constituents (for instance H, H_2, H_2O, O, O_2, and O_3), P the total pressure and P_0 the standard pressure 10^5 Pa.

Table 2-1. Thermodynamic models for solution phases.

Phases	Model	Formula
Gas	Ideal gas	(H_1, H_2, O_1, O_2, O_3, H_2O_1, …)[ii]
Liquid	Substitutional solution with associates	(Cu, H, O, S, P, Cu_2S, Cu_2O)
FCC_A1	2-sublattice model	$(Cu, S, P)_1(O, H, Va^i)_1$

i. Va stands for vacancy. The FCC_A1 phase is used to describe both the metallic solution phase and oxide/hydride phases.
ii. Parantheses separates sublattices in the thermodynamic model.

For liquid metal, different kinds of models are available to describe its thermodynamic properties. In this work, the liquid metal is of low interest and could be omitted. To be able to describe equilibria with almost pure liquid copper, a simple thermodynamic model with few parameters will be used. The associate model for liquid assumes fictive species in the liquid, such as Cu_2O and Cu_2S (Krull et al. 2000). This makes it possible to describe the strong variation of the liquidus temperature with composition in these systems. With use of Cu_2S and Cu_2O associates, the Gibbs energy per mole becomes (for i = Cu, S, P, H, O, Cu_2S, and Cu_2O):

$$G_m^{liq} = \sum \mathrm{y}\ {}^{o}G_i + RT(\sum y_i ln\, y_i) + \sum_{j>i}\sum y_i y_j L_{ij} \qquad (2\text{-}3)$$

where y is the site fraction and ${}^{O}G_i$ the Gibbs energy of individual constituents in the liquid state, $RT(\Sigma y_i ln\ y_i)$ is the ideal entropy of mixing, and $\sum_{j>i}\sum y_i y_j L_{ij}$ the lowest order interaction term between different species and can be expanded in a Redlich-Kister polynomial, giving both temperature and compositional dependencies (Lukas et al. 2007).

The solid solution of hydrogen, oxygen, sulphur and phosphorus in copper is described for the FCC phase with a two-sublattice model (Sundman and Ågren 1981, Hillert 2001). The first sublattice contains substitutional elements (i = Cu, S, and P), and the other sublattice interstitial elements plus vacancies (j = H, O, and Va). The Gibbs energy can then be expressed for two sublattices:

$$G_m^{FCC} = \sum\sum y_i' y_j''\ {}^{o}G_{i:j} + RT\left(\sum y_i' ln\, y_i' + \sum y_j'' ln\, y_j''\right) + {}^{E}G_m \qquad (2\text{-}4)$$

where y_i' and y_j'' are the site fractions on each sublattice, and ${}^{E}G_m$ is the excess term in similarity with the interaction term given in Eq. (2-3), although it becomes more complex since interaction on each sublattice gives many possible interaction terms (Lukas et al. 2007).

2.2 Estimating thermodynamic properties

Those phases that are to be part of the thermodynamic calculations must have a defined Gibbs energy. By definition, the thermochemical properties of a phase are tabulated at 298.15 K in various types of handbooks. The main interest in this work is low temperature equilibria at temperatures close to 298.15 K. For this reason, extrapolations in temperature are not always of greatest concern. On the other hand, it is often of interest to evaluate equilibria at high temperatures. The low mobility of many elements in copper at room temperature gives slow phase transformations. For this reason high temperature equilibria can be taken as an indication of the low-temperature microstructure. To allow for this, the Gibbs energies must be given with a good temperature description.

In practice, tabulated heat capacity, entropy, enthalpy or Gibbs energy is used to evaluate the temperature stability of stoichiometric phases or end-members of solid solution phases. For some compounds there might be missing thermochemical information that has to be estimated. The heat capacity is often estimated using the Kopp-Neumann rule (Grimvall 1999), meaning that the heat capacity of the compound is set equal to a linear average of the heat capacity of the pure components (end-members). The pure components can be pure elements, but also basic components of complex oxides. Since the heat capacity is calculated from the second derivative of Gibbs energy, this implies that the Gibbs energy of an unknown compound can be estimated from the contribution of the end-members $\Sigma_i b_i G_i$:

$$G_m^{\theta} - \sum_i b_i G_i = a + bT \qquad (2\text{-}5)$$

a and b are coefficients to be evaluated. Tabulated values of entropy and Gibbs energy or enthalpy at 298.15 K are then used to estimate the a and b term in the Gibbs energy expression.

For those substances or phases that lack basic thermochemical information such as Gibbs energy, enthalpy or entropy, the thermal stability has to be estimated. The stability of a complex compound can be estimated from the stability of its constituting basic compounds. For instance, intermediate or intermetallic phases are often evaluated from the stability of the end-members of the alloying system. This gives per definition a reasonable estimate of the relative stability of the complex compound versus

its end-members. A systematic approach to evaluate the stability of basic compounds for silicate and phosphate minerals has been made by La Iglesia (2009). The stability of these basic units, represented by Gibbs energies, with reference to this work are given in Table 2-2. This approach will be used when no information on Gibbs energy is found in literature. In order to prove the accuracy of this method the reported stability of different Cu-P-O-H compounds that will be studied in this work is compared to the estimated stability using the basic units, see Table 2-3. The Gibbs energies in these tables are given relative the pure elements. It can be seen that the agreement is quite good for all compounds.

Table 2-2. Gibbs energy of formation of the basic units at 298.15 K (La Iglesia 2009). The energies are given relative the pure elements in formula units.

Basic unit	Gibbs energy kJ/mol
P_2O_5	–1,637.4
CuO	–136.04
H_2O	–239.59

Table 2-3. Calculated free energy of different Cu-P-O-H compounds at 298.15 K, based on the basic units given in Table 2-2. Literature references are Vieillard and Tardy (1984), Magalhães and Jesus (1986) and Puigdomenech and Taxén (2000). The energies are given relative the pure elements in formula units.

Compound	Gibbs energy kJ/mol	
	Estimate	Literature
$Cu_3(PO_4)_2$	–2,045.5	–2,066.2
$Cu(OH)_2$	–375.6	–360.0
$Cu_2PO_4(OH)$ *Libethenite*	–1,210.1	–1,228.8
$Cu_3PO_4(OH)_3$ *Cornetite*	–1,586.2	–1,600.9
$Cu_5(PO_4)_2(OH)_4$ *Pseudomalachite*	–2,797.0	–2,840.3
$Cu_3(PO_4)_2 \cdot 2H_2O$	–2,524.7	–2,564.8
$Cu_3(PO_4)_2 \cdot 3H_2O$	–2,764.3	–2,753.0

3 Thermodynamic evaluation

3.1 Cu-P

The Cu-P binary system has been studied several times in the past, for instance by Hansen and Anderko (1958), Chandrasekaran (1987), An Mey and Spencer (1990), Subramanian and Laughlin (1994), Miettinen (2001), and Noda et al. (2009). Some of these studies have reported model parameters, and their descriptions will be compared in this work. The main focus in previous studies has been on the copper-rich part of the binary system with phosphorus contents up to the phosphide Cu_3P. This region of the system includes the eutectic reaction of liquid forming copper rich FCC and Cu_3P phase. The phosphide has been modelled as a stoichiometric phase in previous works, and no compositional variation for this phase has been reported.

The calculated phase diagram, using the description by Noda et al., is presented in Figure 3-1. Experimental data is taken from older experimental works, which are used in all previous thermodynamic evaluations (Heyn and Bauer 1907, Lindlief 1933, Mertz and Mathewson 1937, Crampton et al. 1940). Beside these experiments, the liquid phase is quite well studied with reported solubility of phosphorus in equilibrium with phosphorus gas. Thermochemical data for the Cu_3P phase exists, although older data seem to be inconsistent as reported by An Mey and Spencer (1990). Complementary high-temperature data were produced by Noda et al. (2009), which clarified the scatter in thermochemical data.

The phosphorus solubility in FCC-copper is given in higher magnification in Figure 3-2. Calculations are made using four different thermodynamic descriptions (Chandrasekaran 1987, An Mey and Spencer 1990, Miettinen 2001, Noda et al. 2009). It can be seen that the different descriptions give very different extrapolations down to room temperature on the solubility of phosphorus in copper. The presented phase diagram is given in mole-fraction. The corresponding solubility in mass fraction at 25°C is: An Mey and Spencer 386 ppm, Noda et al. 510 ppm, Chandrasekaran 1,080 ppm, and Miettinen 2,900 ppm.

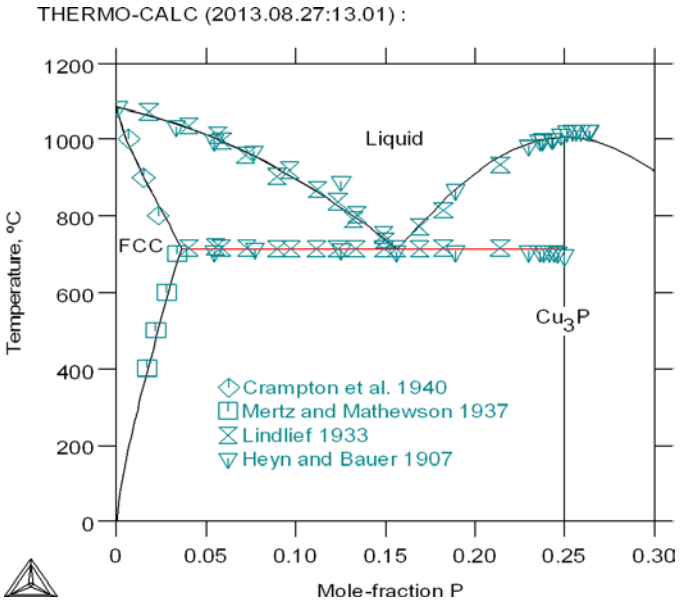

Figure 3-1. *Calculated Cu-rich part of the Cu-P phase diagram. The calculation is made using the thermodynamic description from Noda et al. (2009).*

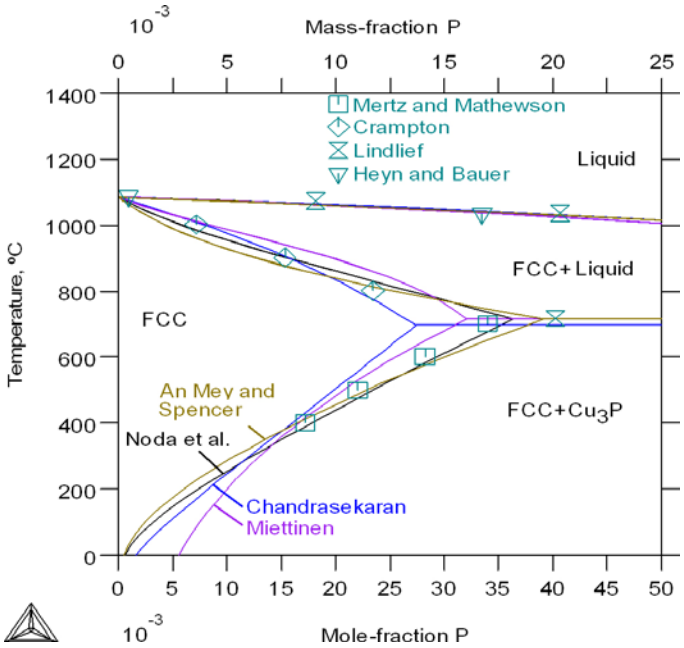

Figure 3-2. *Cu-rich corner of Cu-P phase diagram, calculated using different descriptions.*

The solubility of phosphorus is calculated from the interaction of phosphorus and copper atoms in FCC and the stability of the Cu_3P phosphide in relation to the FCC phase. Comparing the previous assessments, quite different parameters for both Cu_3P phosphide and the Cu-P interaction in FCC have been used. The different assessments have used interaction parameters with temperature dependencies. Their choices of parameters directly influence the shape of the phase diagram and the extrapolation to lower temperatures. For instance, the work of Miettinen who used the largest positive interaction parameter shows the steepest solubility curve of phosphorus in copper, as seen in Figure 3-2.

Different descriptions for the Cu_3P phosphide have also been used. The calculated enthalpy of formation of Cu_3P is –26.3 kJ per mole of atoms, when using the description by Noda et al. This value can be compared with experiments found in literature giving –18.4 and –27.9 kJ per mole of atoms (Kubaschewski and Alcook 1979, Gordienko and Viksman 1985). Comparative values using other descriptions are –37.8 with Miettinen, –31.3 Chandrasekaran et al., and –22.8 using Mey et al. Additional thermochemical data were produced by Noda et al. at high temperature. The description by Noda et al. reproducesthe thermochemical data well both at low and high temperatures. In addition, their description can best describe the measured solubilities of phosphorus in copper. For these reasons, the description by Noda et al. will be accepted and used in this work. All parameters are given in the Appendix.

3.2 Cu-S

Lee et al. (2007) have published a thermodynamic evaluation of the Cu-S system. This evaluation was made together with an existing description of the Fe-S system, in order to explain experimental information of sulphides in steel. The relative stability between the iron-copper sulphide and the manganese sulphide was discussed. Lee et al. based their evaluation on a detailed experimental summary given by Chakrabarti and Laughlin (1983). The reported stable phases for this system are liquid, copper (FCC), pure sulphur (Monoclinic and Orthorhombic), different Cu_2S morphologies: digenite, α- and β-chalcocite, djurleite ($Cu_{1.93}S$), anilite ($Cu_{1.75}S$), and covelite (CuS). Within the range of the present work, the phases of main interest are FCC, and Cu_2S phases. The calculated Cu-rich part of Cu-S phase diagram is presented in Figure 3-3. The calculation is made using the description by Lee et al., and experimental data is taken from the Cu-S review. The phase boundaries are reasonably well described, including experimental data down to room temperature. The transformation temperatures of the three-phase equilibria are well described, see Table 3-1.

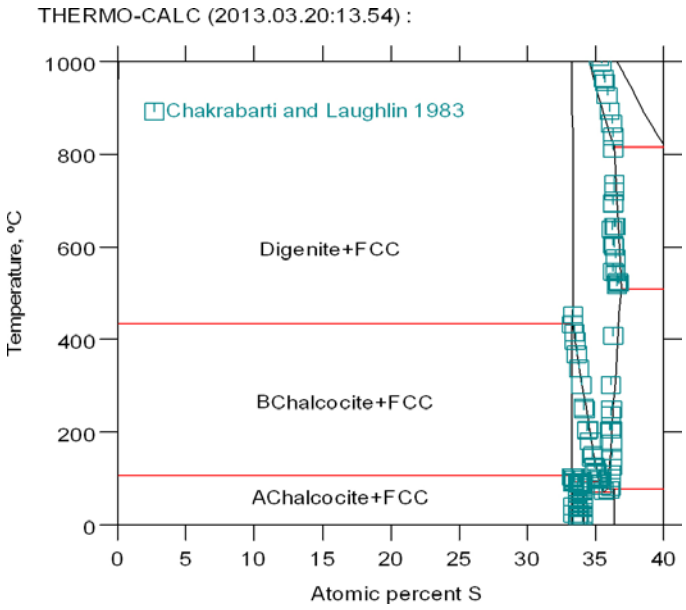

Figure 3-3. *Cu-S binary system up to 40 at% sulphur, according to the description by Lee et al. (2007). Experimental data on phase boundaries and phase transformations have been gathered from many references as summarised in the work by Chakrabarti and Laughlin (1983). AChalcocite and BChalcocite refers to α-Chalcocite and β-Chalcocite, respectively.*

Table 3-1. Calculated transformation temperatures of three-phase equilibria including FCC phase. Literature data summarised in an experimental evaluation of the Cu-S system by Chakrabarti and Laughlin is given as well.

	Calculated (°C)	Chakrabarti and Laughlin (1983) (°C)
L = FCC + Digenite	1,069	1,067
FCC + Digenite = β – Chalcocite	435	435
FCC + β – Chalcocite = α – Chalcocite	106	103.5

The solubility of sulphur in copper is very low. This is shown in the low-temperature regime in Cu-rich phase diagram in Figure 3-4. At 600°C the solubility is calculated to 3.8 atomic ppm (1.9 mass ppm), which is in agreement with experimental data. The solubility at lower temperatures is an extrapolated calculation resulting from the Cu-S interaction in the FCC structure, in relation to the stability of the FCC phase and the Cu_2S phases. Experimentally determined phase boundaries and thermochemical data for the Cu_2S sulphides exist, and have been used by Lee et al. in their evaluation. Standard Gibbs energy of formation of low-temperature Cu_2S (α-chalcocite) is calculated to –91.1 kJ per formula unit Cu_2S. This value shows reasonable agreement to reported numbers at –90.4 to –84.1 kJ per mole (Chakrabarti and Laughlin 1983).

The Cu-S interaction in the FCC phase was given a negative temperature dependence by Lee et al (${}^0L^{fcc}_{Cu,S:Va} = -102200 - 26.5T$), which could give complications when extrapolating sulphur solubility in FCC to low temperatures. In order to evaluate the influence of this temperature dependence a new calculation was made without this temperature dependence with a recalculated interaction parameter. This new parameter was set equal to that used by Lee et al. at 800°C. It can be seen in Figure 3-4 that without this negative temperature dependence the FCC phase has become a little more stable with slightly higher sulphur solubility. The solubility has increased more than one order of magnitude. However, the absolute value of this solubility is still extremely low and cannot be verified experimentally. It is reasonable to conclude that the solubility at room temperature is so low that practically all added sulphur will be found in some sort of inclusion. The sulphur solubility is calculated to 1 mass ppm at 550°C. The evaluation by Lee et al. will be accepted in the present work. All parameters are given in the Appendix.

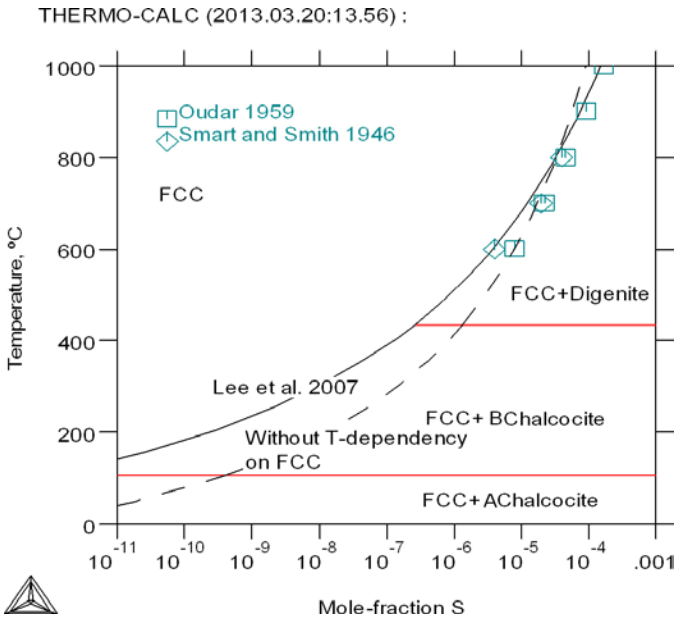

Figure 3-4. *Calculated Cu-rich part of Cu-S phase diagram. Calculation according to the description by Lee et al. (2007), and their description but without temperature dependence on the Cu-S interaction in FCC phase. Experimental data from Smart and Smith (1946) and Oudar (1959).*

3.3 Cu-O

Several different thermodynamic descriptions of the Cu-O system are available in literature. The main differences between these studies are the thermodynamic models used for the liquid phase, and if oxygen is treated as an interstitial or substitutional element in the FCC structure. Schmid (1983), Boudene et al. (1992), and Clavaguera-Mora et al. (2004) have used the associate model for the liquid to describe the Cu-rich part of the Cu-O system. Hallstedt et al. have used the ionic two-sublattice model to describe the liquid in the whole Cu-O system (Hallstedt et al. 1994, Hallstedt and Gauckler 2003). Schramm et al. (2005) have continued on the model by Hallstedt et al., by extending the Cu-O system to very high pressures. Oxygen in FCC-copper is treated as an interstitial element in recent evaluations (Hallstedt and Gauckler 2003, Schramm et al. 2005), and substitutional in other evaluations (Hallstedt et al. 1994, Clavaguera-Mora et al. 2004). In this work, oxygen in FCC will follow the reassessment by Hallstedt and Gauckler (2003) and will be treated as an interstitial element. The liquid metal is given little attention in the present work and the less complicated associate model for liquid will be used, in similarity with the Cu-S system.

A good prediction of the separation between a low-oxygen and a high-oxygen melt (miscibility gap) was made by Clavaguera-Mora et al. using a single interaction parameter with the associate model for liquid. In this work, it was realised that a good description could be achieved by using Cu_2 and Cu_2O associates. By using the Cu_2-Cu_2O associates the critical point in the miscibility gap was close to $x_{Cu} = 0.2$, rather than 0.25 if using the more traditional Cu-Cu_2O associates. However, it will become difficult to combine models where the liquid is modelled with both Cu and Cu_2 as pure copper end-members. As mentioned before, equilibria involving the liquid state are of less interest in the present work, and the Cu-Cu_2O associates will be used. New thermodynamic parameters for the Cu-Cu_2O interaction in the liquid have been evaluated in this work, and are given in the Appendix.

The calculated copper-rich part of the Cu-O system is shown in Figure 3-5. Experimental data is taken from Clavaguera-Mora et al. (2004). The liquidus, with the first solidified Cu_2O and FCC, is well described for low oxygen contents. The Cu-O system shows many similarities with the Cu-S system: low solubility of the element in FCC copper, the presence of a Cu_2O (or Cu_2S) phase, and a miscibility gap in the liquid.

The FCC parameter for copper with all interstitial sites filled by oxygen ${}^{\circ}G^{fcc}_{Cu:O}$, and the Gibbs energy expression for pure Cu_2O are taken from the evaluations by Hallstedt et al. (1994) and Hallstedt and Gauckler (2003). The calculated heat of formation and calculated Gibbs energy of formation for Cu_2O

agree well with experimental data from different references. For instance, the calculated heat of formation for Cu_2O at 298.15 is –170 kJ per formula unit Cu_2O. This value can be compared to experimental values from five different references in the range –165 to –180 kJ per mole (Hallstedt et al. 1994).

Figure 3-6 shows the calculated solubility of oxygen in FCC-copper. The experimental data is taken from (Horrigan 1977, Narula et al. 1983, Hammer et al. 1984, Zhang et al. 1987). Older measurements exist, although these show a significant scatter as pointed out by Hallstedt et al. (1994). The accepted description in this work follows Hallstedt et al. for FCC and Cu_2O, however, the model by Clavaguera-Mora et al. gives nearly identical values. The experimental data shown in Figure 3-6 indicate that the solubility measured in mole-fraction reaches sub-ppm levels already at 600°C, which is even lower than the solubility of sulphur in copper, see Figure 3-4. The solubility at room temperature is much lower than 10^{-12}, and it can be concluded that all oxygen in copper will be found in oxides, inclusions, or other compounds.

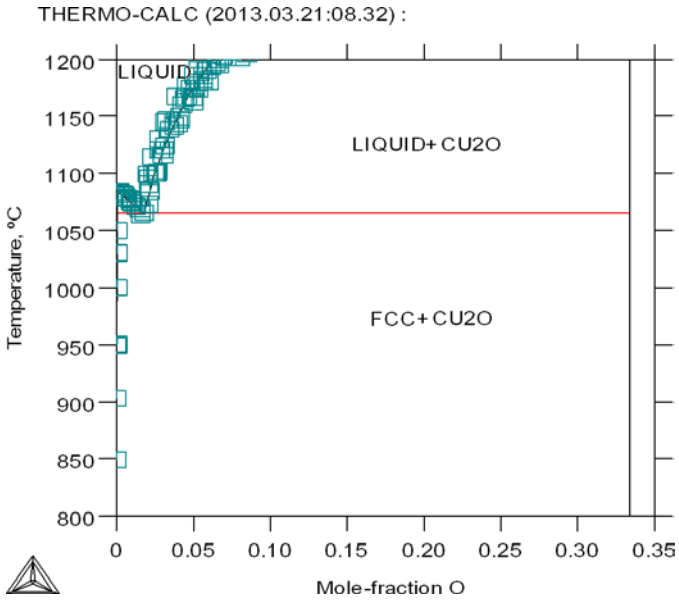

Figure 3-5. *Cu-rich part of Cu-O phase diagram. Experimental data is taken from Clavaguera-Mora et al. (2004).*

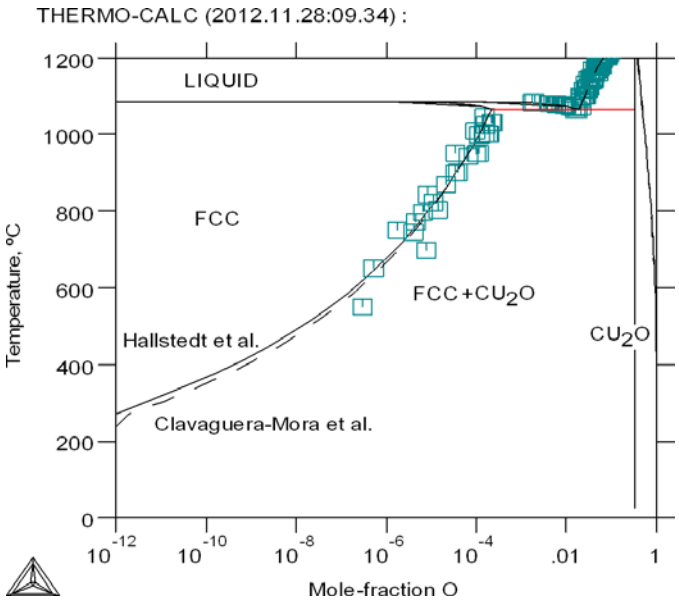

Figure 3-6. *Solubility of oxygen in copper. Experimental data is taken from Horrigan (1977), Narula et al. (1983), Hammer et al. (1984) and Zhang et al. (1987). Thermodynamic description of Cu-O FCC and Cu_2O is taken from Hallstedt and Gauckler (2003), and compared with description by Clavaguera-Mora et al. (2004).*

3.4 Cu-H

3.4.1 Previous work on Cu-H system

The Cu-H system consists of three stable phases at atmospheric pressure, FCC, gas, and liquid. The binary phase diagram can be found in older references, such as Hansen and Anderko (1958), Lyman (1973), and Massalski (1986). All these references rely on the same experimental data and give similar or identical phase diagrams. Much of the experimental work up to the 1970s are summarised in these evaluations.

The only thermodynamic evaluation available in literature for Cu-H is the work by Huang et al. (2007), as a part of the ternary Cu-Pd-H system. The main focus was the Pd side of the system and to evaluate the influence of copper additions on the hydrogen solubility in Pd-Cu alloys. The experimental data used for the Cu-H system were limited to solubility curves at 50 MPa hydrogen pressure. Due to lack of experimental data for Cu-H, ternary data was used to fit the Cu-H system.

3.4.2 Experimental information

Solid copper has a very low solubility of hydrogen. This solubility increases with temperature and reaches a maximum at the liquidus of 0.01 at% at 1,357 K (Lyman 1973). Not many direct measurements on the hydrogen solubility at low temperatures exist in literature. Measurements have been made by McLellan, who determined the hydrogen solubility by a hot extraction technique of quenched samples (McLellan 1973). Newer experiments are due to Sverchkova et al. (1989) who studied the hydrogen solubility down to 450°C. They used degasification techniques to evaluate the amount of dissolved hydrogen in copper. The measured solubility close to 400°C gives a solubility of 1 atomic ppm, which corresponds to 0.016 mass ppm. Caskey et al. (1975) have measured the tritium content in 99.999 % pure copper exposed to tritium gas at 1 atm pressure for 260 hours at 262°C. The tritium content was measured by liquid scintillation counting of solutions obtained by acid dissolution of specimen. The tritium content was determined to be approximately 0.0003 mass ppm ($2 \cdot 10^{-8}$ atom ppm), which is a similar value to McLellan if extrapolating high temperature data. In this work, no difference will be made between tritium and hydrogen solubilities. Older experiments from Röntgen and Möller (1934), Lieser and Witte (1954), Eichenauer and Pebler (1957), and Thomas (1967) have been taken from the work by McLellan (1973).

Estimates on the solubility of hydrogen in copper at even lower temperatures are mainly calculated values based on evaluated hydrogen permeability. By applying a hydrogen pressure on one side of a thin copper foil, the build-up of a hydrogen pressure on the vacuum side can be evaluated as a function of the permeating hydrogen atoms. The permeability, and the amount of hydrogen diffusing through the thin foil, is put equal to the product of hydrogen solubility and hydrogen diffusivity. With this approach it is possible to estimate the solubility at low temperatures. Begeal (1978) studied the permeability at 220–440°C, with hydrogen pressures at 0.01–1.4 atm H_2. The hydrogen pressure was continuously measured on the vacuum side of the membrane. In a similar manner, Tanabe et al. (1984) reported solubilities evaluated at 230–930°C and 0.01–1 atm pressure. Considerable scatter has been reported when using this technique, and permeability data will not be used in this evaluation.

Copper in equilibrium with hydrogen gas has been reported to obey Sievert's law, with solubility proportional to the square root of the pressure. For instance, Shapovalov (1999) verified this relation at 600–1,100°C and 1–1,000 atm H_2 pressure, and Sverchkova et al. (1989) at 450–700°C and 0.1–1 atm pressure. Since many experiments are made at different hydrogen pressures, Sievert's relation makes it possible to compare these experiments independently of pressure.

There is no stable copper hydride in the Cu-H system at atmospheric pressure (Lyman 1973, Massalski 1986). However, metastable copper hydrides CuH can be formed chemically or electrochemically. Three different hydrides are included in this work: the hexagonal CuH (wurtzite type), cubic CuH hydride with hydrogen in tetrahedral positions (sphalerite type), and cubic CuH with hydrogen in octahedral positions (halite type). In Korzhavyi and Johansson (2010) and Korzhavyi et al. (2012), the thermodynamic properties of the hexagonal copper hydride have been calculated from first principles and compared with reported information in literature. The experimental data is mainly from Burtovyy and Tkacz (2004) and Burtovyy et al. (2003). A cubic polymorph of this hydride taking the sphalerite structure has been calculated as well, and reported to be slightly

less stable (Korzhavyi and Johansson 2010). The stability of the corresponding cubic hydride with hydrogen in octahedral positions (halite structure) has also been calculated by Korzhavyi[1]. This CuH hydride was estimated to have an enthalpy that was approximately 20 kJ/mol higher than the sphalerite type of hydride. The CuH hydride with halite structure corresponds to the FCC-copper with all sites filled with hydrogen, and will be used as an estimate of the ${}^{\circ}G^{fcc}_{Cu:H}$ parameter.

3.4.3 Thermodynamic evaluation

The thermodynamic description of the FCC phase in the Cu-H system has been evaluated. Values for liquid and gas are identical with previous work by Huang et al. (2007). All model parameters are summarised in the Appendix. Input to the assessment has been solubility data of hydrogen in FCC-copper together with calculated stability of FCC-copper with all sites filled by hydrogen (halite structure).

The optimised Cu-H phase diagram is presented in Figure 3-7. The calculations using the optimised and Huang et al. descriptions are compared with the older evaluation found in Metals Handbook (Lyman 1973). The agreement to the older experimental data given in Metals Handbook on the maximum solubility in FCC and liquid phase is good.

The solubility of hydrogen in FCC-copper in the low temperature regime is shown in Figure 3-8. The calculation according to the optimisation made in this work is compared with the description by Huang, the empirical relation by McLellan, and experimental data with references given in figure. The empirical relation of McLellan is given as mole-fraction hydrogen as $x_H = 0.011exp\,(-6.62 \cdot 10^3/T)$, which is nearly identical to the expression used by Martinsson et al. (2013). It can be seen that the optimised set of parameters in this work gives a lower solubility of hydrogen in FCC-copper compared to the previous assessment. The difference is three orders of magnitude at 200°C and increases with lower temperature. The empirical relation by McLellan is nearly identical with the present work, and could be used as an approximation of the hydrogen solubility in copper.

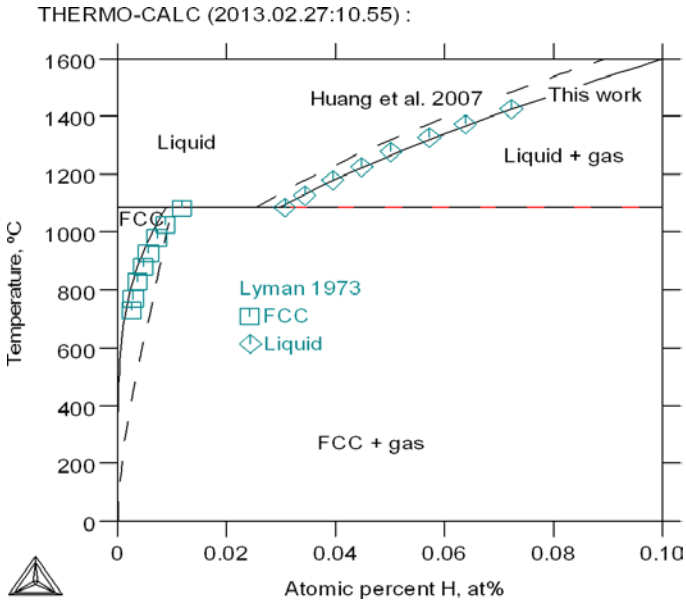

Figure 3-7. *Calculated Cu-H phase diagram according to this work, work by Huang et al. (2007), and Lyman (1973).*

[1] Unpublished work by Korzhavyi P A (2005) at KTH Royal Institute of Technology, Stockholm, Sweden.

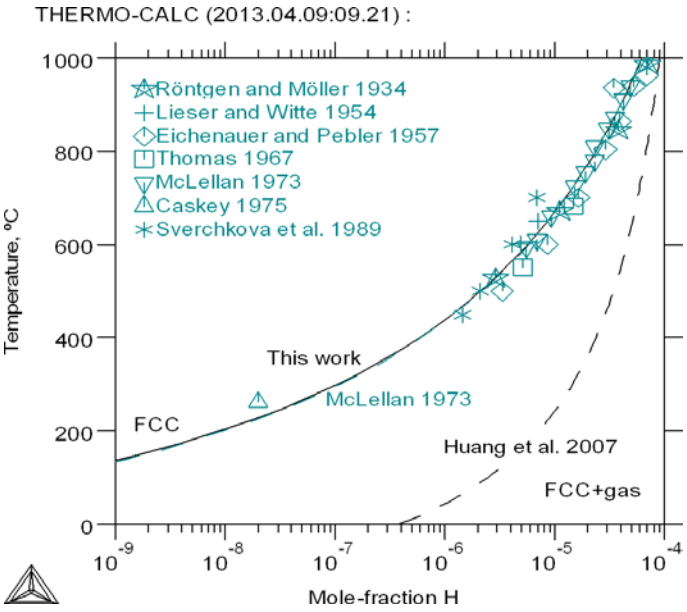

Figure 3-8. *Calculated Cu-H phase diagram focusing on the solubility of hydrogen in FCC-copper. Experimental data from Röntgen and Möller (1934), Lieser and Witte (1954), Eichenauer and Pebler (1957), Thomas (1967), McLellan (1973) and Sverchkova et al. (1989). Calculations are made at 1 atm pressure.*

The estimated stability of the FCC-copper with all sites filled with hydrogen (halite type of CuH) was taken from the unpublished work by Korzhavyi (2005). The enthalpy was used as input in the optimisation but allowed to vary slightly to give the best fit to solubility data. The final value was 61 kJ/mol in enthalpy, calculated from the elements and given per formula unit CuH. The stability of hexagonal CuH (wurtzite) and the other cubic CuH (sphalerite) have been taken directly from the work by Korzhavyi and Johansson (2010). The most stable copper hydride is the hexagonal copper hydride. The calculated solubility limit in the FCC structure before hydride precipitation is 29 mass ppm. This will require an unrealistic high pressure to raise the hydrogen content in the FCC-structure, to avoid the gas phase, and to get copper hydride precipitation. As comparison, the hydrogen content in the FCC structure at atmospheric pressure and 298.15 K is as low as $3 \cdot 10^{-8}$ mass ppm.

3.5 Thermodynamic evaluation of higher systems

3.5.1 Stoichiometric compounds and thermodynamic data

Many different compounds exist in the Cu-H-O-S-P system. These are different phosphorus sulphides, sulphates, and phosphates, existing both with and without copper. The addition of hydrogen will give rise to many new crystalline compounds that have been included in the thermodynamic description. Most of the hydrogen compounds are based on oxygen compounds. The strong relation between oxygen and hydrogen is important to keep in mind when discussing hydrogen contents in various copper grades. A stable hydrogen compound for OFP-copper could be a possible explanation for the high hydrogen content that has been measured for these materials, which far exceeds the hydrogen solubility of hydrogen in FCC-copper. The stability of these stoichiometric compounds will be evaluated in this chapter.

The solubility of hydrogen, oxygen, sulphur and phosphorus in copper has been evaluated in the binary systems. All ternary interaction parameters are set to zero. Ternary element interaction in solid copper is expected to be of less importance at low temperatures. This is due to the low concentration of these elements in copper, and the thermodynamic impact of element interaction is proportional to its concentration. It is thus a good approximation in the present work to set the ternary interaction parameters to zero. The solubility of oxygen in FCC-copper is extremely low. In the binary phase diagrams the solubility of oxygen reached ppm levels already at 600°C, see Figure 3-6. It will be shown in this section that the stability of higher ordered stoichiometric oxygen-compounds will further lower this solubility. The sulphur solubility is also low in FCC-copper due to the presence

of sulphides. Above 800°C, sulphides are not stable and the sulphur content will be in solution. At these temperatures, a possible sulphur-phosphorus interaction could be expected in the FCC-structure. However, no experimental information about this ternary interaction can be found in literature, and the parameters are set to zero.

The thermodynamic data needed to evaluate the stability of different stoichiometric compounds have been taken from different thermochemical handbooks: NIST-JANAF (Chase 1998), Barin and Knacke (1973), Barin et al. (1977), The NBS tables (Wagman 1982), Vieillard and Tardy (1984), Knacke et al. (1991). Hereafter, these references will be referred to as thermochemical handbooks.

3.5.2 Stoichiometric compounds in Cu-O-S-P system

Many stable phosphorus sulphides exist, and some of these also show an order-disorder transformation. An experimentally determined P-S binary phase diagram is given by Okamoto (1991). The following P-S phases have been reported: P_2S_5 (α and β), P_4S_9, P_4S_7 (α and β), P_4S_5, PS, P_4S_3 (α and β), and P_2S. The following P-S phases have been evaluated using data in thermochemical handbooks: P_4S_5, P_2S_5, P_4S_3, and P_4S_7. The remaining phases PS, P_2S and P_4S_9 could not be evaluated due to lack of experimental information. Of these phases, both PS and P_2S are low temperature phases. P_4S_9 is stable up to the liquidus although both the evaluated phases P_2S_5 and P_4S_7 are stable to higher temperatures. For this reason, the most stable P-S compounds have been taken into consideration.

The quasi-binary system Cu_2S-P_2S_5 has been experimentally studied by Blachnik et al. (1991). The following phases were reported: Cu_7PS_6, Cu_3PS_4, and $(CuPS_3)_n$. The compound $Cu_4P_2S_7$ has also been reported, although it could not be verified by Blachnik et al. No thermochemical information about these phases can be found in literature, and the phases are therefore not evaluated in this work. The possibility that they will be stable in OFP-copper can still be evaluated. For instance, the copper phosphorus sulphide Cu_7PS_6 calculated from the following relation, ${}^\circ G_{(cr)}^{Cu_7PS_6} = 3.5{}^\circ G_{(cr)}^{Cu_2S} + 0.5{}^\circ G_{(cr)}^{P_2S_5}$, would require a large negative contribution to the Gibbs energy (–250 kJ/mol) to become stable. This would give a completely wrong appearance of the quasi-binary Cu_2S-P_2S_5 system reported by Blachnik et al. (1991). For this reason, it is unlikely that any Cu-P-S compound should become stable for OFP-copper.

The following Cu-S-O sulphates have been included: Cu_2SO_4, $CuSO_4$, and $CuO{\cdot}CuSO_4$. Gibbs energy expressions for the latter two were evaluated using data from Puigdomenech and Taxén (2000). Cu_2SO_4 was tabulated by Puigdomenech and Taxén but has been reevaluated using data from Shishin and Decterov (2012) in order to have a more detailed temperature dependence. Both expressions yield similar values at 298.15 K.

The following Cu-P-O phosphates have been studied: P_4O_{10}, $Cu_2P_2O_7$, and $Cu_3(PO_4)_2$. The stability of the pentaoxide P_2O_5 (denoted P_4O_{10}) has been evaluated based on tabulated data in thermochemical handbooks. The thermochemical properties of the diphosphate $Cu_2P_2O_7$ have been studied by Le et al. (2008). The diphosphate exists in two polymorphs, a low-temperature α-$Cu_2P_2O_7$ that transforms to a high-temperature β-$Cu_2P_2O_7$ at a temperature of about 350 K. The thermochemical properties of these two polymorphs are similar, and they will be treated as one phase. No heat capacity data could be found for this compound. The enthalpy of formation has experimentally been determined from the oxides CuO and P_2O_5 (P_4O_{10}), with reported value of –279 kJ/mol. This equals an enthalpy of –2,091 kJ/mol calculated from the elements. The Gibbs energy of the $Cu_2P_2O_7$ phosphate at 298.15 K is estimated from the following relation ${}^\circ G_{298.15}^{Cu_2P_2O_7} = a_i + b_iT + 2{}^{est}G_{298.15}^{CuO} + {}^{est}G_{298.15}^{P_2O_5}$. The superscript *est* refers to the tabulated data at 298.15 K of the basic units given in Table 2-2. The evaluated enthalpy of –2,091 kJ/mol, will be used together with an estimate of the Gibbs energy based on the basic units. The calculated Gibbs energy is –2,169 kJ/mol, which is in agreement with a reference giving –2,132 kJ/mol (–1,874 kJ/mol when calculated from the elements) (La Iglesia 2009). This approach yields entropy per atomic mole of 27.1 J/mol,K, which is similar to the better documented copper phosphate $Cu_3(PO_4)_2$ that is 28.5 J/mol,K (Puigdomenech and Taxén 2000).

The phosphate $Cu_3(PO_4)_2$ was evaluated in the work by Puigdomenech and Taxén (2000). However, a simplified expression was used to describe the heat capacity. The following expression is now used for the phosphate ${}^\circ G_{(cr)}^{Cu_3(PO_4)_2} = a_i + b_iT + 3{}^\circ G_{(cr)}^{CuO} + 0.5{}^\circ G_{(cr)}^{P_4O_{10}}$. The coefficients are calculated using tabulated values for entropy and Gibbs energy of formation at 298.15 K. The calculated heat capacity agrees very well with tabulated data. At 298.15 K the reported value is 229.0 J/mol,K (Puigdomenech and Taxén 2000), which can be compared to the calculated value 232.5 J/mol,K.

3.5.3 Stoichiometric compounds in Cu-H-O-S-P system

The following Cu-H-O compounds will be included in the present description: Cu-H cubic and hexagonal (see Chapter 3.4.3), CuOH, and $Cu(OH)_2$. Cupric hydroxide $Cu(OH)_2$ has been evaluated using thermochemical data tabulated in thermochemical handbooks (Chase 1998) and gives identical Gibbs energy of formation at 298.15 K to Puigdomenech and Taxén (2000). Korzhavyi et al. have used quantum-mechanical calculations to determine the stability of CuOH (Korzhavyi and Johansson 2010). The enthalpy and Gibbs energy of formation from the elements are given at 298.15 K as ΔG= –158.2 kJ/mol and ΔH = –199.8 kJ/mol. These values were used to evaluate the temperature stability of CuOH, calculated from the elements.

Some different hydrated copper sulphates and hydroxides have been evaluated, which appear as stable minerals in nature:

- Poitevinite $CuSO_4 \cdot H_2O$
- Bonattite $CuSO_4 \cdot 3H_2O$
- Chalcanthite $CuSO_4 \cdot 5H_2O$
- Langite $CuSO_4 \cdot 3Cu(OH)_2 \cdot H_2O$
- Antlerite $CuSO_4 \cdot 2Cu(OH)_2$
- Brochantite $CuSO_4 \cdot 3Cu(OH)_2$

Hydrated copper sulphates on the formula $CuSO_4 \cdot xH_2O$ have been evaluated using tabulated heat capacity temperature functions, entropy, and Gibbs energy of formation at 298.15 K found in thermochemical handbooks. The copper sulphate hydroxides have been estimated from the following relations: $^\circ G_{(cr)}^{CuSO_4 \cdot xCu(OH)_2} = a_i + b_i T + {}^\circ G_{(cr)}^{CuSO_4} + x\,{}^\circ G_{(cr)}^{Cu(OH)_2}$ and $^\circ G_{(cr)}^{CuSO_4 \cdot 3Cu(OH)_2 \cdot H_2O} = a_i + b_i T + {}^\circ G_{(cr)}^{CuSO_4 \cdot H_2O} + 3\,{}^\circ G_{(cr)}^{Cu(OH)_2}$, where the coefficients *a* and *b* are fitted to tabulated Gibbs energy and entropy at 298.15 K.

The thermodynamic properties of the hydrogen compound $Cu_3(P_2O_6OH)_2$ have been studied by Le et al. (2008). The enthalpy of formation was determined to –4,302.7 kJ/mol. A similar approach as for $Cu_2P_2O_7$ will be used, with Gibbs energy at 298.15 K estimated as $^\circ G_{298.15}^{Cu_3(P_2O_6OH)_2} = a_i + b_i T + 3\,{}^{est}G_{298.15}^{CuO} + 2\,{}^{est}G_{298.15}^{P_2O_5} + {}^{est}G_{298.15}^{H_2O}$, according to the procedure given in Chapter 2.2. The estimated Gibbs energy at 298.15 K, measured enthalpy, and stoichiometric average for heat capacity are all used to express the Gibbs energy of $Cu_3(P_2O_6OH)_2$.

The following Cu-H-P-O copper phosphate hydroxides can be found as stable minerals in nature:

- Libethenite $Cu_2PO_4(OH)$
- Cornetite $Cu_3PO_4(OH)_3$
- Polymorphs of $Cu_5(PO_4)_2(OH)_4$ such as pseudomalachite, reichenbachite, and ludjibaite.

The temperature dependency of the Gibbs energy expressions for these minerals have been estimated to follow the copper phosphate and copper hydroxide according to the following relation $^\circ G^{Cu_{3x+y}(PO_4)_{0.5x}(OH)_{0.5y}} = a_i + x\,{}^\circ G^{Cu_3(PO_4)_2} + y\,{}^\circ G^{Cu(OH)_2}$. The coefficient *a* is fitted to reported Gibbs energy of formation at 298.15 K by Magalhães and Jesus (1986), which is in agreement with estimated energies, see Table 2-3. No information on the stability of reichenbachite or ludjibaite could be found in literature. In addition, no further thermochemical information on the entropy part could be found in literature. The heat capacity of pseudomalachite has been reported to be 383 J/mol,K (Bissengaliyeva et al. 2012), which can be compared with the calculated value of 411 J/mol,K. The heat capacity of libethenite has been reported as 142 J/mol,K (Belik et al. 2011), and the calculated value is 164 J/mol,K.

Two different hydrated copper phosphates will be included, these are:

- $Cu_3(PO_4)_2 \cdot 2H_2O$
- $Cu_3(PO_4)_2 \cdot 3H_2O$

In similarity to other compounds, the Gibbs energy for these hydrated copper phosphates will be estimated from the following relation ${}^{\circ}G_{(cr)}^{Cu_3(PO_4)_2 \cdot xH_2O} = a_i + b_i T + {}^{\circ}G_{(cr)}^{Cu_3(PO_4)_2} + x{}^{\circ}G_{(g)}^{H_2O}$. Puigdomenech and Taxén (2010) have tabulated Gibbs energy and entropy for $Cu_3(PO_4)_2 \cdot 3H_2O$, which have been used. The reported Gibbs energy at 298.15 K is in agreement with estimates, see Table 2-3, and in accordance with data in other references (Vieillard and Tardy 1984, La Iglesia 2009). The approach used yields a heat capacity at 298.15 K of 333 J/mol,K, compared to 351 J/mol,K given in (Puigdomenech and Taxén 2000). No entropy or heat capacity could be found for $Cu_3(PO_4)_2 \cdot 2H_2O$. In this work it will be assumed that both these minerals have the same entropy per mole of atoms. This value, together with tabulated Gibbs energy at 298.15 K (La Iglesia 2009), is used to evaluate the coefficients.

3.6 Gases Cu-H-O-S-P

The stability of many different gas molecules has been evaluated. Their Gibbs energy expressions are given in Appendix. In general, tabulated data given in NIST-JANAF (Chase 1998) and Barin and Knacke (1973) have been used. Inconsistent thermochemical data for Gibbs energy have been reported for the P_4O_6 gas. Tabulated values are around –2,247 kJ/mol (Chase 1998), whereas other report –1,606 kJ/mol (Knacke et al. 1991), and –1,883.7 kJ/mol (Glaum et al. 1991). However, it is known that heating P_4O_6 gas at temperatures 200–250°C should decompose into other gaseous phosphorus oxides and solid phosphorus (red) (Bailar et al. 1973). By making equilibrium calculations at atmospheric pressure, only the two less negative Gibbs energies will allow for this reaction. In this work, the suggested value –1,883.7 kJ/mol will be used.

4 Equilibrium calculations for OFP-Cu

4.1 Thermodynamic calculations

In the previous chapter, a thermodynamic description for the Cu-H-O-S-P system was evaluated. In this chapter, this thermodynamic description will be used to calculate equilibria for OFP-copper. The equilibrium phases and their compositions will be evaluated. In addition, those phases that are not stable can be evaluated and put in relation to the stable phases to discuss their possible significance for OFP-copper. The influence of the different elements in OFP-copper, hydrogen, oxygen, sulphur and phosphorus, will be studied. Calculations for OFP-Cu will have a typical composition of 50 ppm phosphorus, 6 ppm sulphur, 3 ppm oxygen and 0.35 ppm hydrogen (Andersson et al. 2004, SKB 2006, 2010).

Equilibrium calculations will first be made on OFP-copper without hydrogen, and then including hydrogen as well. It will be shown that the measured hydrogen content in commercial OFP-copper far exceeds the hydrogen content in solid solution plus possible hydrogen in crystalline compounds. Hydrogen storage in different crystalline defects such as dislocations, grain boundaries, cavities, vacancies etc, is not included in the thermodynamic model. For this reason, the complicated nature of hydrogen in copper will be presented and discussed separately.

4.2 Equilibrium calculations without hydrogen

The calculated equilibrium of copper with 50 ppm phosphorus, 6 ppm sulphur and 3 ppm oxygen is shown in Figure 4-1 as a function of temperature. The different morphologies of Cu_2S (α, β-chalcocite, and digenite) are nearly identical in stability and the sulphur solubility in FCC phase will remain at low levels below 550°C. The most stable oxygen-compound is the copper phosphate $Cu_2P_2O_7$. Its high stability makes it precipitate from the liquid. The sulphur content in the matrix reaches ppm levels at 554°C, and lower temperatures will further lower this solubility. The oxygen content is at ppm levels slightly below solidus, with the solidification of the final melt, due to the presence of the copper phosphate. Most of the phosphorus content remains in solid solution and a minor part of the 50 ppm is found in the copper phosphate. The equilibrium phases remain stable below 600°C, if disregarding the different crystal structures of the stoichiometric Cu_2S sulphide.

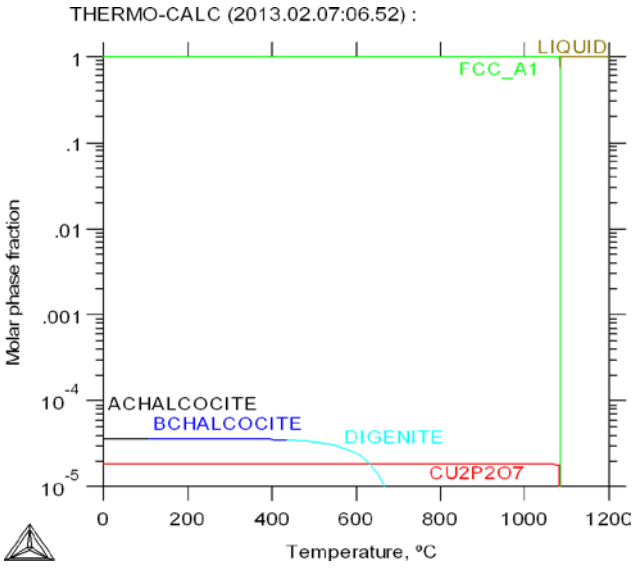

Figure 4-1. *Calculated equilibrium for copper with 50 ppm phosphorus, 6 ppm sulphur and 3 ppm oxygen.*

The influence of phosphorus in OFP-copper is demonstrated by making equilibrium calculations for a phosphorus-free copper with 6 ppm sulphur and 3 ppm oxygen in Figure 4-2. It can be seen that without phosphorus, the copper oxide Cu_2O is the stable oxygen compound. Its stability is not as high as the phosphate and oxygen is allowed to remain in solid solution above 800°C. Due to the stoichiometry of the copper oxide, the phase fraction is twice as high for OF-copper due to more copper atoms per oxygen in Cu_2O, compared to copper plus phosphorus atoms per oxygen atoms in $Cu_2P_2O_7$.

The driving force for precipitation is calculated for many different Cu-O-S-P phases, as shown in Figure 4-3. The driving force can be seen as the relative stability versus the stable phases in the system, and is normalised against RT (where R is the gas constant and T temperature). A zero value implies a stable phase, and a value slightly below zero indicates its possible presence in equilibrium calculations. The P-S phases (P_4S_3, P_4S_5, P_4S_7, P_2S_5) have a very negative driving force far from becoming stable and is therefore not shown in figure. The different Cu_2S morphologies are all similar in stability and close to zero below 700°C. The $Cu_2P_2O_7$ phase is stable at all temperatures. The other

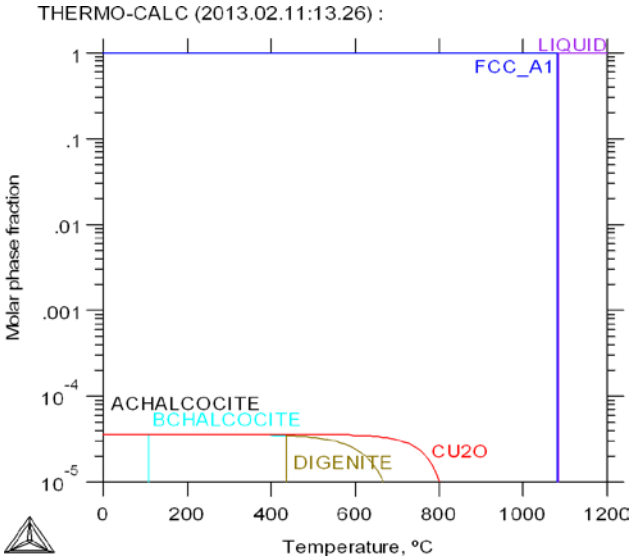

Figure 4-2. *Calculated equilibrium for copper with 6 ppm sulphur and 3 ppm oxygen.*

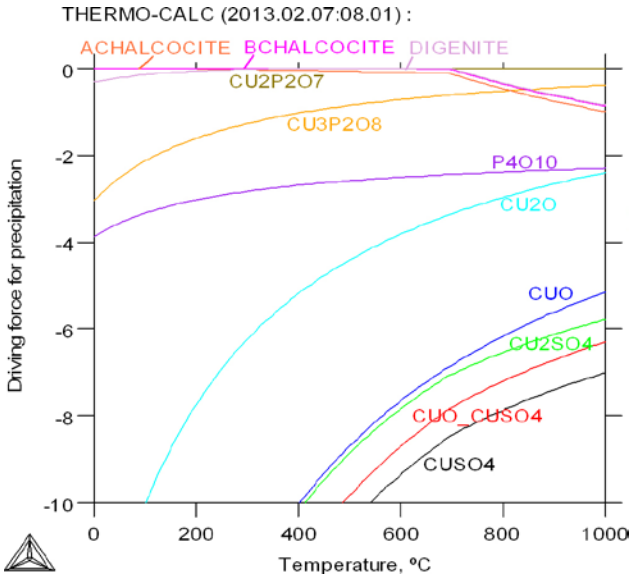

Figure 4-3. *Driving force for precipitation calculated for copper with 50 ppm phosphorus, 6 ppm sulphur, and 3 ppm oxygen. The driving force is the relative stability of different phases, normalised against RT and therefore dimensionless.*

copper phosphate $Cu_3(PO_4)_2$ and phosphate P_4O_{10} are both more stable than Cu_2O oxide. The copper sulphates (Cu_2SO_4, $CuO{\cdot}CuSO_4$, and $CuSO_4$) cannot compete with the copper sulphide about the sulphur due to their much lower stability.

The different equilibrium phases are evaluated for high contents of sulphur and phosphorus using 3 ppm oxygen and 298.15 K in Figure 4-4. It can be seen that no new phase will appear if the sulphur content is increased. On the other hand, if the phosphorus content is increased above approximately 500 ppm, the copper phosphide Cu_3P will precipitate.

A part of the phosphorus content will be used to form the phosphates. Focus on the low-phosphorus region for copper with 3 ppm oxygen and 6 ppm sulphur at 298.15 K is shown in Figure 4-5. It can be seen that the transition to $Cu_2P_2O_7$ occurs approximately at 0.5 times the oxygen content. At lower phosphorus contents, the Cu_2O oxide will be stable together with the other copper phosphate $Cu_3(PO_4)_2$. This phosphate becomes stable due to higher oxygen to phosphorus relation, which is advantageous in a phosphorus deficient region.

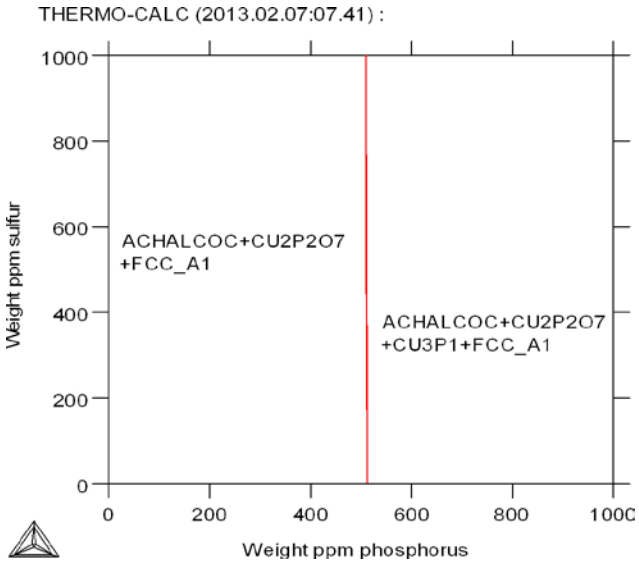

Figure 4-4. *Equilibrium phases for copper with 3 ppm oxygen and different contents of phosphorus and sulphur. The calculation is made at 298.15 K.*

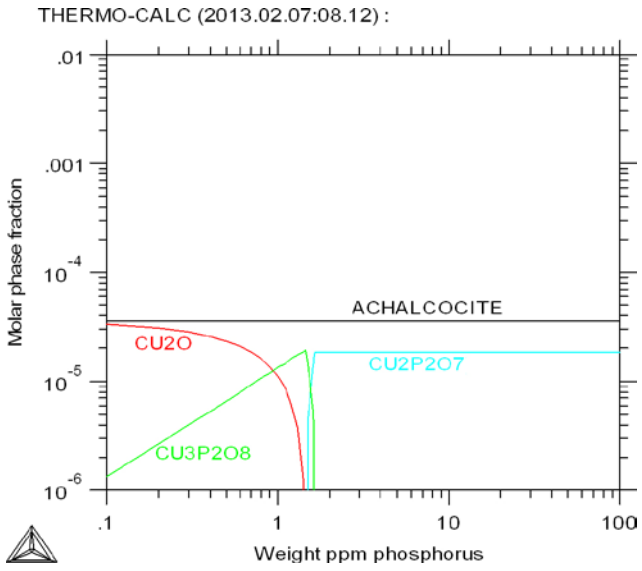

Figure 4-5. *Calculated equilibrium as function of phosphorus content for copper with 3 ppm oxygen and 6 ppm sulphur at 298.15 K.*

Equilibrium calculations with increasing oxygen content are made for copper with 50 ppm phosphorus and 6 ppm sulphur at 298.15 K, as shown in Figure 4-6. This type of calculations can be made to illustrate the oxide scale that can be found on copper in contact with atmosphere. The CuO oxide is stable at the highest oxygen partial pressures, for instance air. With lower oxygen content, and further away from the atmosphere, the type of oxide will gradually change to Cu_2O oxide. Even lower oxygen contents will give separate oxide islands in a FCC-copper matrix. The $Cu_3P_2O_8$ phosphate is calculated stable due to its higher oxygen to phosphorus relation. In similarity, the Cu_2S to $CuO{\cdot}CuSO_4$ transition will occur at high oxygen contents due to higher oxygen to sulphur relation. This type of equilibrium calculations often gives the correct type of phases in the oxide scale. However, since some elements are more easily oxidised, compositional variations in the oxide scale is often seen. Since phosphorus has a much higher affinity to oxygen than copper, it is likely that phosphorus could accumulate close to the surface.

Some experimental studies on phase equilibria for OFP-copper exist in literature. Savolainen (2012) has studied the microstructure of friction stir welded OFP-copper. Inclusions were found in the microstructure, which were identified with EDS-analysis to be rich in sulphur. The welded material had smaller sulphides, which was believed to be due to the elevated temperature causing dissolution of sulphides. Typical FSW-temperatures were reported to be 800–900°C. The dissolution of sulphides is shown in Figure 4-1, to take place above 700°C. Sulphur rich inclusions have also been reported by Pakarinen (2011) using TEM. No P-rich inclusions or oxides were reported in these studies.

Phosphorus is known to have a very strong influence on the conductivity (Davis 2001). Smart and Smith (1946) studied the influence of phosphorus on the conductivity of oxygen-free and oxygen containing copper. Copper without oxygen showed a clear decrease in conductivity as function of phosphorus additions. On the other hand, the copper with oxygen present did not show any significant loss in conductivity with phosphorus content. This clearly indicates the strong deoxidising properties of phosphorus in copper , and that phosphates should be more stable than copper oxides. The type of phosphate was never clarified by Smart and Smith, but were possibly P_4O_{10}, $Cu_2P_2O_7$, or $Cu_3(PO_4)_2$.

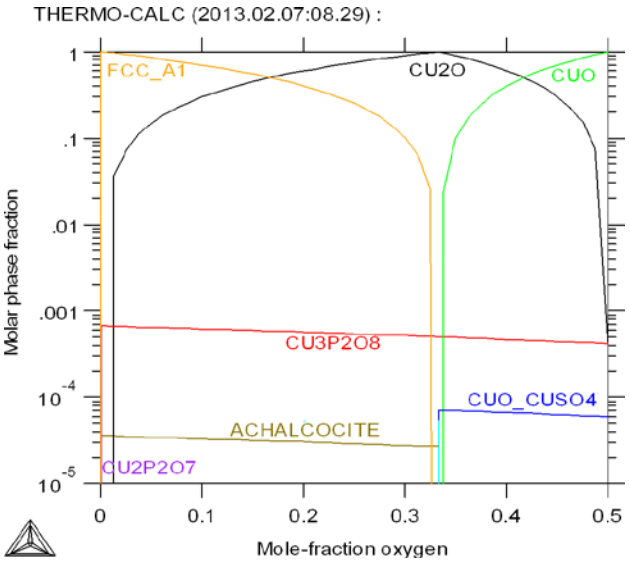

Figure 4-6. *Calculated stable phases as function of oxygen content, calculated at 298.15 K for 6 ppm sulphur and 50 ppm phosphorus.*

4.3 Equilibrium calculations with hydrogen

The calculated isoplethal section of OFP-copper with 50 ppm phosphorus, 6 ppm sulphur, 3 ppm oxygen, and varying hydrogen content is shown in Figure 4-7. The corresponding hydrogen isoactivity lines are shown as well, with hydrogen activity 1 corresponding to an atmospheric pressure of hydrogen. Higher activities are approximately the square root of the hydrogen pressure (in atm), according to Sievert's law. The different low-temperature morphologies of the copper sulphide are not shown in the figure, and all these sulphides are given as Cu_2S. It can be seen in the figure that the copper phosphates are present already at 1,000°C. The type of phosphate depends on the hydrogen content, with increasing hydrogen content giving $Cu_3(P_2O_6OH)_2$ instead of $Cu_2P_2O_7$. Below 700°C the sulphide will become stable, independently of the hydrogen content. With lower temperature the hydrogen content in the FCC phase decreases and 0.1 ppm in OFP-copper is reached already at 600°C, when including the hydrogen content in the phosphate $Cu_3(P_2O_6OH)_2$.

The isoactivity lines give valuable information on the hydrogen-behaviour of OFP-copper. It can be seen that in such a harsh environment as pure hydrogen gas the hydrogen solubility in OFP-copper is very low, and much lower than typical contents in OFP-copper (approximately 0.35 ppm). A reasonable explanation for this is that hydrogen is captured in crystalline defects such as vacancies, dislocations, grain boundaries, porosity etc, which are not taken into account in the thermodynamic model. At equilibrium with hydrogen gas, the copper phosphates are stable against reduction. Increasing the hydrogen activity from 1 to 10 increases the hydrogen solubility at high temperatures. The main difference between the low activities to the high activities (100 and 1,000) is that the copper phosphate can be reduced as well, giving water as main hydrogen-oxygen compound.

The measured hydrogen content in OFP-copper far exceeds the solubility in the matrix phase at atmospheric pressure. In addition, no crystalline phase including a high content of hydrogen is stable at these conditions. Nevertheless, calculations will be made on OFP-copper including 0.35 ppm hydrogen, and thereby forcing hydrogen to be in some phase (excluding gaseous hydrogen). This will correspond to a high pressure and high hydrogen activity. The calculated equilibria of copper with 50 ppm phosphorus, 6 ppm sulphur, 3 ppm oxygen, 0.35 ppm hydrogen is shown in Figure 4-8 as function of temperature. The calculations correspond to a hydrostatic pressure that exceeds the atmospheric pressure, as will be shown and discussed later. At high temperature hydrogen is in solid solution, and oxygen is found in the copper phosphate $Cu_2P_2O_7$. The solubility of hydrogen in copper decreases with lower temperature, and hydrogen is then found in other phases: $Cu_3(P_2O_6OH)_2$ and aqueous water.

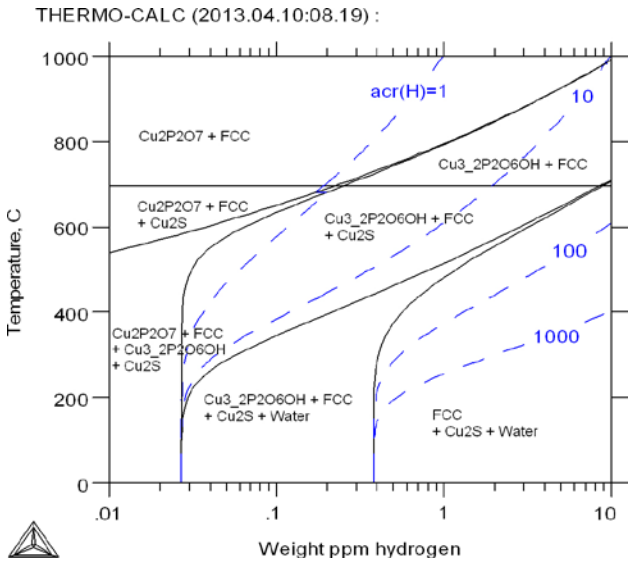

Figure 4-7. *Calculated phase stability for copper with 50 ppm phosphorus, 6 ppm sulphur, 3 ppm oxygen and varying hydrogen content. The corresponding isoactivity lines for hydrogen are shown as well.*

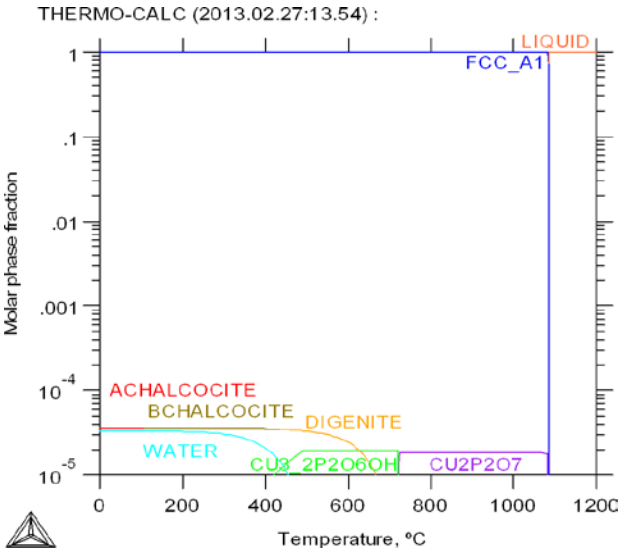

Figure 4-8. *Calculations made for copper with 50 ppm phosphorus, 6 ppm sulphur, 3 ppm oxygen and 0.35 ppm hydrogen. The calculations are made without the gas phase.*

The corresponding hydrostatic pressure needed to raise the hydrogen content in the material to 0.35 ppm is shown in Figure 4-9. This pressure is compared with the pressure needed to suppress water vapour to aqueous water. It can be seen that the pressure increases from room temperature at 150 atm up to 600 atm at 400°C for OFP-copper. There is therefore a strong driving force for hydrogen to form gas in the crystalline material, for example in cavities.

Equilibrium calculations at atmospheric pressure, allowing for gaseous hydrogen in the material, will now be made. Equilibrium calculations for OFP-copper are shown in Figure 4-10, giving phase fractions as a function of temperature. The copper phosphate $Cu_3(P_2O_6OH)_2$ is very similar in stability to the copper phosphate $Cu_2P_2O_7$. As previously shown, the solubility of hydrogen decreases with temperature, and the 0.35 ppm hydrogen used in calculations exceeds the solid solution content below approximately 800°C. At intermediate temperatures 400–800°C, hydrogen will be found in gas as H_2/H_2O mixture. Below 400°C, the copper phosphates become stable again causing a gradual transition from water vapour rich gas to nearly pure hydrogen gas. At room temperature, nearly all oxygen is in the copper phosphates and the gas is more or less pure hydrogen gas. The different copper phosphates are very similar in stability, and it is likely that the high-temperature $Cu_2P_2O_7$ could remain to low-temperature service.

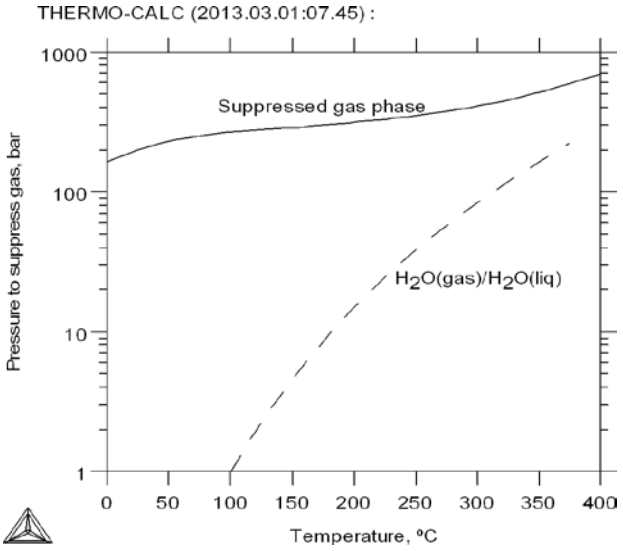

Figure 4-9. *Pressure needed to suppress the gas phase in equilibrium calculations made for copper with 50 ppm phosphorus, 6 ppm sulphur, 3 ppm oxygen and 0.35 ppm hydrogen.*

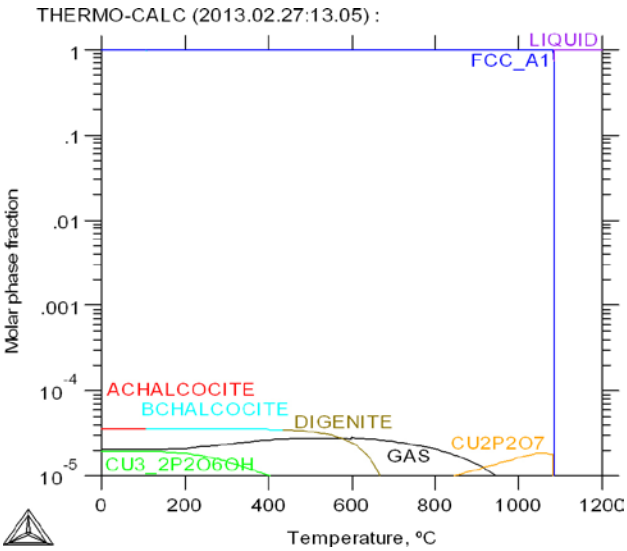

Figure 4-10. *Calculated equilibrium for Cu with 50 ppm phosphorus, 6 ppm sulphur, 3 ppm oxygen, 0.35 ppm hydrogen.*

A similar calculation for OF-copper at atmospheric pressure gives another appearance, see Figure 4-11. For OF-copper, no phosphorus is available to form phosphates and water or water vapour will be the dominating hydrogen-oxygen compound. As a consequence, any present Cu_2O oxide could be reduced by hydrogen and possibly embrittle the material by forming water vapour. In similarity with phosphorus OFP-copper, sulphur is still found in its copper sulphide, rather than forming any hydrous copper sulphate.

The constitution of the gas phase in equilibrium with OFP-copper is shown in Figure 4-12a, and OF-copper in Figure 4-12b. It can be seen, that the presence of a low-temperature copper phosphate that solve the oxygen (see Figure 4-10) gives a hydrogen rich gas at low temperatures. On the other hand, OF-copper with copper oxides that are not stable against hydrogen reduction will give water vapour rich gas phase at temperatures below 400°C.

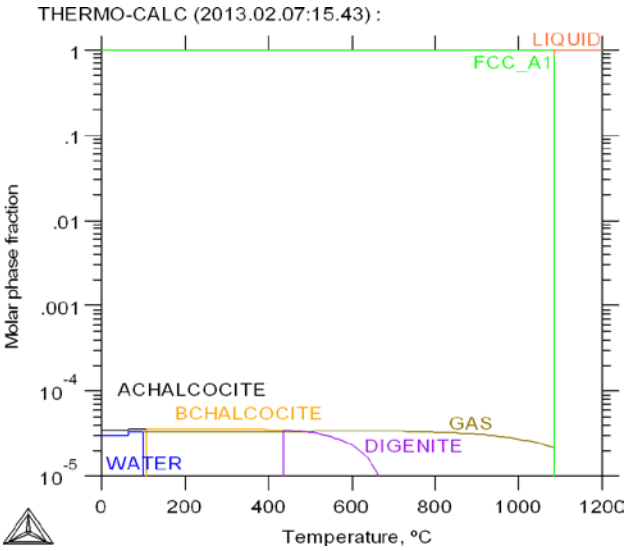

Figure 4-11. *Calculated equilibrium for Cu with 6 ppm sulphur, 3 ppm oxygen, 0.35 ppm hydrogen, but without phosphorus.*

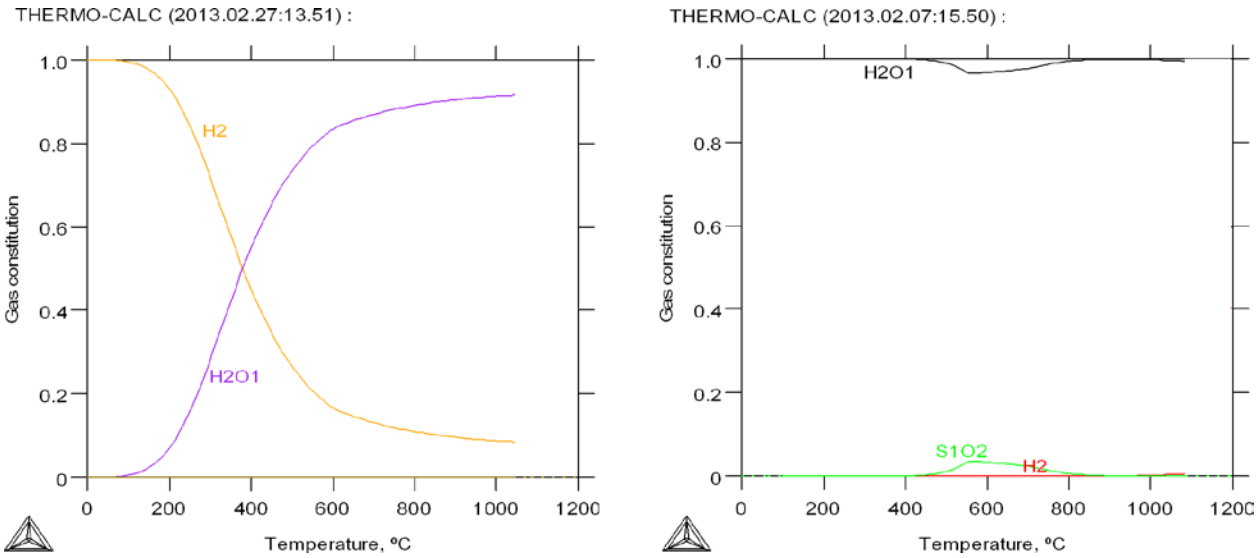

Figure 4-12. *Constitution of gas phase for a) OFP-copper (conditions according to Figure 4-10a) b) OF-copper (conditions according to Figure 4-11).*

The calculated content of hydrogen, oxygen, sulphur and phosphorus in FCC-copper is shown in Figure 4-13. The calculation is made for copper with 50 ppm phosphorus, 6 ppm sulphur, 3 ppm oxygen, and 0.35 ppm hydrogen at both 1 atm and 150 atm hydrogen pressure. It can be seen that the solubility of oxygen is extremely low in the presence of phosphorus, compared to the Cu-O binary phase diagram. The solubility of sulphur and hydrogen are also low, whereas the main part of phosphorus is in solid solution. The solubility of hydrogen in FCC-copper is higher than both oxygen and sulphur at room temperature. The solubility of hydrogen is also pressure dependent, since hydrogen is present in the gas phase.

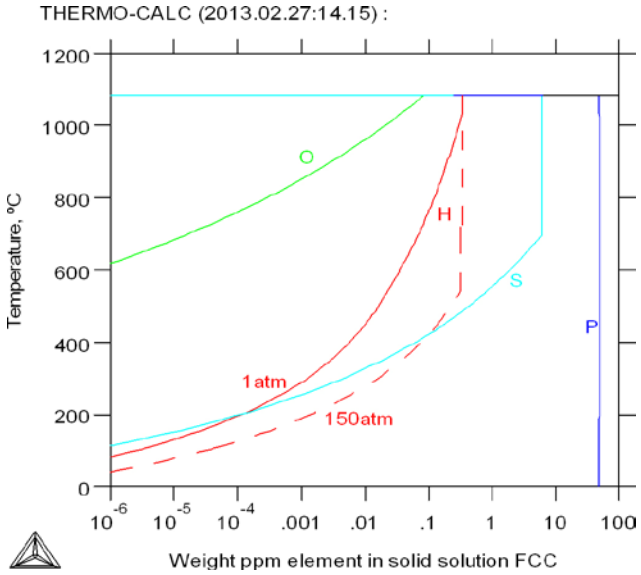

Figure 4-13. *Solubility of H, O, S, P in FCC-copper, calculated for a system containing copper and 50 ppm phosphorus, 6 ppm sulphur, 3 ppm oxygen and 0.35 ppm hydrogen. Calculations are made at both 1 atm and 150 atm pressure.*

The hydrogen content of thermally charged OFP-copper in hydrogen gas at 1 atm pressure has been studied by Martinsson et al. (2013). The charging was evaluated at both 600 and 675°C, with results given in Table 4-1. These results are compared with a reference sample of as-received copper and compared with calculations on copper with 50 ppm phosphorus, 6 ppm sulphur, and 1.5 ppm oxygen at 1 atm hydrogen gas (Martinsson et al. 2013). No hydrogen-compound is calculated as stable at these high temperatures, and all calculated hydrogen is in solid solution in FCC phase. The calculated contents are lower than these measurements. On the other hand, the calculations are in good agreement with other solubility data according to the Cu-H binary system, see Figure 3-8. The calculation gives the amount of hydrogen in solid solution, without any hydrogen trapped in crystalline defects. It should therefore be seen as a lower limit when comparing with commercial OFP-copper.

The possible stability of $Cu(OH)_2$ is evaluated by a calculated isoplethal section shown in Figure 4-14. This hydroxide is not stable in the temperature-pressure range. Instead, copper oxides plus water vapour or aqueous water are stable phases. The same results are found for the cuprous hydroxide, CuOH.

Table 4-1. Hydrogen content in OFP-copper compared with equilibrium calculations. Values are given in mass ppm.

	Martinsson et al. 2013	Equilibrium calculation of H in solid solution at 1 atm pressure
Reference	0.68±0.12	
675°C/1 h	0.72±0.11	0.06
600°C/10 h	0.36±0.07	0.04

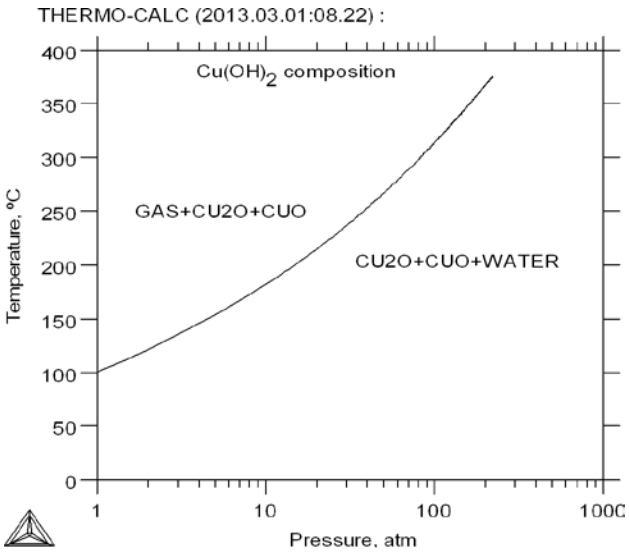

Figure 4-14. *Temperature-pressure chart calculated for $Cu(OH)_2$ compositions.*

5 Discussion

In this work, all binary systems including copper that belong to the Cu-H-O-S-P system have been evaluated. Thermodynamic assessments given in literature have been reviewed and compared. In some cases improvements have been needed, for instance in the Cu-H and Cu-O systems. The solubility of hydrogen in copper has been raised several orders of magnitude at room temperature with the new description for Cu-H. This has been made possible with the combined use of ab-initio calculated stabilities and a careful evaluation of experimental data of the Cu-H system.

In addition, many different stoichiometric compounds have been evaluated for higher systems as well. The evaluated thermodynamic description allows for multicomponent equilibrium calculations for OFP-copper. This makes it possible to determine the solid solution of elements in copper, compare the relative stability of different phases, and to evaluate the impact of a temperature or compositional change of OFP-copper on the equilibrium. The results in previous chapters will be discussed below.

Sulphur in copper forms sulphides. It is unlikely that other sulphur-compound should form at typical OFP-copper compositions; the Cu_2S sulphides are much more stable than other sulphur compounds. It has been shown in this work that phosphorus-sulphides are unlikely to form. Copper containing phosphorus sulphides have been reported in literature, although these were found to have a considerable lower stability than the pure copper sulphide. At high partial pressure oxygen, such as an oxide scale, sulphates can become stable instead of copper sulphide.

In this work 6 ppm sulphur has been used in calculations. Adding more sulphur will simply result in more copper sulphides rather than any other Cu-H-O-S-P compound. Sulphur is therefore not expected to cause any dramatic change in material properties with increasing content. Higher content will simply and proportionally result in more sulphides. Sulphides are often believed to lower the ductility and it could be desirable to minimise the sulphur content. However, creep testing of OFP-copper with different sulphur contents (6 and 12 ppm) has not shown any negative effect on creep properties (Andersson-Östling and Sandström 2009). The stable sulphides at creep testing will be the stable sulphides at long-term use of OFP-copper. The design limit of 12 ppm of sulphur seems well motivated and experimentally studied.

Phosphorus has a high affinity to oxygen. It has been shown how several different phosphates are more stable than copper oxide Cu_2O. These are $Cu_2P_2O_7$, $Cu_3(PO_4)_2$, and P_4O_{10}. Phosphates have also been found to compete with hydrogen about the oxygen content, and both $Cu_2P_2O_7$ and $Cu_3(P_2O_6OH)_2$ were found more stable than water vapour below 300°C at any pressure, and more stable than water up to approximately 200 atm pressure. Copper phosphates that form at high temperatures could remain stable to low temperatures, depending on the hydrogen activity in the material. Phosphorus-free copper shows the opposite behaviour, copper oxides that form at high temperature will get reduced by hydrogen at low temperature.

Phosphorus might form phosphates together with oxygen, although the major part of phosphorus will be found in solid solution. As a simple estimate, 0.5 times the oxygen content in mass is consumed by phosphates. Oxygen in OFP-copper is typically present in a few ppm. The solubility limit of phosphorus in copper falls with decreasing temperature. At 298.15 K the solubility limit is calculated to 510 ppm in equilibrium with the phosphide Cu_3P. Phosphorus has shown a very positive effect on the creep properties of OFP-copper compared with OF-copper on both creep strength and creep ductility, mainly at temperatures below 300°C (Andersson-Östling and Sandström 2009). The influence of phosphorus on copper from a thermodynamic analysis makes it possible to conclude that the major part of phosphorus will be found in solid solution, a minor part of phosphorus can be consumed by phosphates, and phosphates are stable against hydrogen reduction below 300°C at atmospheric pressure and elevated pressure. The specified design limits for phosphorus are well inside this solubility limit, and far above the phosphorus content consumed by phosphates at the oxygen levels specified for the OFP-copper used by SKB.

The calculated solubility of hydrogen in solid solution versus the measured hydrogen content in OFP-copper indicates an excess amount of hydrogen in the material. This has been shown experimentally by 10 hours exposure in hydrogen gas at 600°C and 1 atm pressure which lowered the hydrogen content

of OFP-copper compared to the reference material (Martinsson et al. 2013), see Table 4-1. This is an important finding, since it can be concluded that the high hydrogen content in OFP-copper can be remaining from the material processing at high temperatures. This hydrogen content is therefore not thermodynamically stable at atmospheric pressure, and should leave the material depending on the kinetics of the reaction. For this reason, it is not unexpected that the calculated hydrogen in OFP-copper is mainly found in gaseous species. No crystalline phase has been found explaining this high hydrogen content.

Equilibrium calculations for a crystalline defect-free material allows for omitting the gas phase in calculations. The needed pressure to suppress the gas is depending on the hydrogen and oxygen content of the material. Calculations for OFP-copper with 3 ppm oxygen and 0.35 ppm hydrogen give a pressure at room temperature of 150 atm (~15 MPa) to fully suppress the gas phase, which mainly consists of hydrogen gas. However, defects in the crystalline lattice such as voids, dislocations, grain boundaries and cavities are possible sites for hydrogen storage and it is unlikely that the material will be exposed to such a high hydrogen activity or hydrogen pressure. It is shown in this work that copper phosphates ($Cu_2P_2O_7$ or $Cu_3(P_2O_6OH)_2$) are more stable than water vapour below 400°C at atmospheric pressure. On the other hand, OF-copper without phosphorus will give water vapour or water at all temperatures and pressures. The water molecule will be more difficult to store in crystalline defects compared to the smaller hydrogen atom and molecule.

Water vapour can be suppressed to aqueous water at high pressures, but hydrogen gas in pure copper cannot be avoided at realistic pressures. If oxygen is present, water can form at high hydrogen pressures. If disregarding any crystalline defects in copper, hydrogen will have a theoretical upper limit of 1/8 of the oxygen content based on the hydrogen/oxygen relation of water. Higher hydrogen contents would require very high pressures to avoid hydrogen gas and thereby exceeding the mechanical strength of the OFP-copper, and possibly cause porosity. This has been indicated by experiments on electrolytically charged OFP-copper, with porosity due to extreme conditions with very high hydrogen activity and hydrogen contents (Martinsson et al. 2013).

The small size of the hydrogen atom and its relatively high mobility even at room temperature should be an argument for hydrogen to reach its equilibrium concentration at atmospheric pressure, which is apparently not the case. A reason for this could be the strong interaction between oxygen and hydrogen. Copper when exposed to air will form a thin but dense oxide scale, as calculated and shown in Figure 4-6. Even though internal hydrogen could reduce the copper surface oxides, a continuous supply of oxygen from the environment will hinder hydrogen degassing. The thermal charging at 600°C in hydrogen gas could have reduced the surface oxides, similar to oxide reduction in powder metallurgy, allowing for hydrogen degassing. The strong oxygen-hydrogen interaction on hydrogen charging/degassing has been experimentally demonstrated by Caskey et al. (1975), by charging copper with different content oxygen at 450 K and 535 K. Copper with the highest oxygen content, ETP-copper with 200–400 ppm oxygen, was not charged at 1 atm hydrogen pressure due to oxygen trapping near the surface and required 69 MPa overpressure to charge. On the other hand, copper with lower oxygen contents (less than 10 ppm) was easily charged at atmospheric pressure. Spontaneous hydrogen degassing will be thermodynamically favoured at low temperatures, since the solubility of hydrogen in FCC-copper decrease with decreasing temperature. In addition, an oxygen-free atmosphere with a low partial pressure of hydrogen will further favour this reaction.

Cu-O-H compounds are very unlikely to be found stable. Calculations on $Cu(OH)_2$ resulted in water or water vapour together with copper oxides CuO and Cu_2O. Calculations on copper hydride showed that high hydrogen contents are required to reach the solubility limit of hydrogen in FCC-copper. At 298.15 K the hexagonal copper hydride was found stable at 10 ppm, which is nearly 100 million times higher than the solubility limit of hydrogen in FCC-copper at atmospheric pressure. This will require an unrealistic high pressure or hydrogen activity to suppress the gas phase and reach this high hydrogen content.

6 Conclusions

A thermodynamic evaluation for Cu-H-O-S-P has been made, with special focus on the use of OFP-copper as canister material for spent nuclear fuel. All binary systems including copper have been reviewed. Gaseous species and stoichiometric crystalline phases have been included for higher systems.

Sulphur in OFP-copper:

- Sulphur will be found in sulphides. The sulphide is stable from approximately 700°C down to room temperature. The sulphide could be of different morphologies but constant stoichiometry Cu_2S.
- The solubility of sulphur in FCC-copper is very low, 1 mass ppm is reached already at 550°C and the solubility decreases with decreasing temperature.
- Phosphorus-sulphides, with or without copper, is not calculated as stable for OFP-copper. The copper sulphide is calculated to be much more stable. Copper sulphates could become stable in the oxide scale at high oxygen partial pressures replacing the sulphide.

Phosphorus in OFP-copper:

- Phosphorus has a high affinity to oxygen, and will form phosphates. Calculations at atmospheric pressure with low hydrogen content yields $Cu_2P_2O_7$, and high hydrogen content $Cu_3(P_2O_6OH)_2$.
- Both $Cu_3(P_2O_6OH)_2$ and $Cu_2P_2O_7$ are calculated more stable than water vapour below 300°C at all pressures, and more stable than water below 150 atm pressure calculated for OFP-copper with excess hydrogen.
- For OFP-copper, a minor part of phosphorus is consumed by phosphates and the major part is in solid solution at room temperature. The solubility limit of phosphorus in copper is calculated to 510 ppm at room temperature, in equilibrium with the copper phosphide Cu_3P.

Oxygen in OFP-copper:

- The solubility of oxygen in pure copper is very low, and will be even lower in copper alloyed with stronger oxide forming elements such as phosphorus. For OFP-copper, ppm levels of oxygen in solid solution is reached already at solidus.
- At atmospheric pressure, oxygen will be found in phosphates for OFP-copper. Copper oxides will become stable first when all phosphorus has been consumed, which takes place at twice the phosphorus content (calculated in weight).
- Copper oxide is not stable with excess hydrogen and will be reduced to elementary copper plus water or water vapour. Copper phosphates are stable below 300°C against hydrogen reduction at atmospheric pressure. At high hydrogen activity the phosphates can be reduced as well.

Hydrogen in OFP-copper:

- Commercial OFP-copper has a high content of hydrogen that far exceeds the hydrogen content in solid solution at room temperature and atmospheric pressure. Hydrogen is calculated to be in gaseous form, experimentally verified by degassing of OFP-copper in pure hydrogen at 600°C.
- OFP-copper at overpressure can suppress gas. This hydrostatic pressure is lower than the creep strength of OFP-copper at room temperature, and could explain the high hydrogen content OFP-copper without internal porosity.
- At high hydrogen activities, phosphates can be reduced giving aqueous water. However, copper phosphates are still more stable than water vapour.
- At atmospheric pressure and temperatures above 400°C, no crystalline phase including hydrogen has been found stable for OFP-copper. At low temperatures and atmospheric pressure $Cu_3(P_2O_6OH)_2$ is calculated stable for OFP-copper.
- The solubility of hydrogen in FCC-copper is low. At 675°C, 0.06 ppm hydrogen in FCC-copper is in equilibrium with hydrogen gas at atmospheric pressure.

7 Suggestions for future work

Equilibrium calculations on OFP-copper have highlighted the importance of copper phosphates. These phosphates will replace the less stable copper oxides and give an effect of phosphorus on oxygen-free copper. These phosphates are more stable against hydrogen reduction compared to the copper oxide. Not much experimental data for copper phosphates suitable for thermodynamic evaluations exists in literature. This is probably due to the low content of oxygen in OFP-copper and the reactive nature of oxygen making it difficult to cast model alloys including oxygen and to equilibrate these in the solid state. In addition, copper exposed to oxygen at high partial pressure will produce a dense oxide layer rather than copper phosphates. A possibility could be oxidising OFP-copper at low partial pressure oxygen in a controlled $H_2/H_2O/O_2$ atmosphere. The partial pressure should be low enough to avoid copper oxides but high enough to produce the more stable copper phosphates. This could verify the higher stability of the copper phosphates. Another possibility could be indirect measures, such as verifying older experiments on copper conductivity for copper-phosphorus alloys with and without oxygen.

Commercial OFP-copper contains a hydrogen content that far exceeds the hydrogen solubility in the matrix phase. This is true also for other materials than copper. In this work, no crystalline phase has been found that can explain the high hydrogen content measured for OFP-copper at room temperature and atmospheric pressure. As a consequence, hydrogen should eventually leave the material. Hydrogen degassing should be further studied, and especially in a reducing atmosphere that avoids any surface oxides and possible oxygen-hydrogen interaction that could impede the degassing process.

In this work, the thermodynamics of the Cu-H-O-S-P system has been evaluated making it possible to determine the solubility of hydrogen, oxygen, sulphur and phosphorus in copper and the equilibrium phases. A possible continuation to this work is to evaluate the mobility of these elements in copper. By combining this kinetic information with the thermodynamic description diffusion phenomena of hydrogen, oxygen, sulphur and phosphorus in copper can be studied.

8 Acknowledgements

This work has been financed by Swedish Nuclear Fuel and Waste Management (SKB). Christina Lilja and Matts Björck SKB, Rui Wu Swerea KIMAB, and Pavel Korzhavyi KTH, are all thanked for discussions, comments and interest in the present work.

9 References

SKB's (Svensk Kärnbränslehantering AB) publications can be found at www.skb.se/publications.

An Mey S, Spencer P J, 1990. A thermodynamic evaluation of the copper-phosphorus system. Calphad 14, 265–274.

Andersson C-G, Eriksson P, Westman M, Emilsson G, 2004. Lägesrapport kapseltillverkning. SKB R-04-14, Svensk Kärnbränslehantering AB. (In Swedish.)

Andersson-Östling H C M, Sandström R, 2009. Survey of creep properties of copper intended for nuclear waste disposal. SKB TR-09-32, Svensk Kärnbränslehantering AB.

Bailar J C, Emeléus H J, Nyholm R, Trotman-Dickenson A F, 1973. Comprehensive inorganic chemistry. Vol 2. Ge, Sn, Pb, group VB, group VIB, group VIIB. Oxford: Pergamon Press.

Barin I, Knacke O, 1973. Thermochemical properties of inorganic substances. Berlin: Springer-Verlag.

Barin I, Knacke O, Kubaschewski O, 1977. Thermochemical properties of inorganic substances. Supplement. Berlin: Springer-Verlag.

Begeal D R, 1978. Hydrogen and deuterium permeation in copper alloys, copper-gold brazing alloys, gold, and the in situ growth of stable oxide permeation barriers. Journal of Vacuum Science and Technology 15, 1146–1154.

Belik A A, Naumov P, Kim J, Tsuda S, 2011. Low-temperature structural phase transition in synthetic libethenite Cu_2PO_4OH. Journal of Solid State Chemistry 184, 3128–3133.

Bissengaliyeva M R, Gogol D B, Bekturganov N S, 2012. Low temperature measurements of the heat capacity and thermodynamic functions of pseudo-malachite $Cu_5(PO_4)_2(OH)_4$. Thermochimica Acta 532, 139–144.

Blachnik R, Gather B, Andrae E, 1991. Ternary chalcogenide systems X: the quasiternary system Ag_2S-Cu_2S-P_4S_{10}. Journal of Thermal Analysis 37, 1289–1298.

Boudene A, Hack K, Mohammad A, Neuschütz D, Zimmermann E, 1992. Experimental investigation and thermochemical assessment of the system Cu-O. Zeitschrift für Metallkunde 83, 663–668.

Burtovyy B, Tkacz M, 2004. High-pressure synthesis of a new copper hydride from elements. Solid State Communications 131, 169–173.

Burtovyy B, Włosewicz D, Czopnik A, Tkacz M, 2003. Heat capacity of copper hydride. Thermochimica Acta 400, 121–129.

Caskey G R, Dexter A H, Holzworth M L, Louthan M R, Derrick R G, 1975. The effect of oxygen on hydrogen transport in copper. Corrosion 32, 370–374.

Chakrabarti D J, Laughlin D E, 1983. The Cu-S (copper-sulfur) system. Bulletin of Alloy Phase Diagrams 4, 254–271.

Chandrasekaran L, 1987. Thermodynamic evaluation of Cu-Fe-P-C system. Thermo-Calc AB, Stockholm, Sweden.

Chase M W (ed), 1998. NIST-JANAF thermochemical tables. 4th ed. Woodbury, NY: American Institute of Physics.

Clavaguera-Mora M T, Touron J L, Rodríguez-Viejo J, Clavaguera N, 2004. Thermodynamic description of the Cu-O system. Journal of Alloys and Compounds 377, 8–16.

Crampton D K, Burghoff H L, Stacy J T, 1940. The copper-rich alloys of the copper-nickel-phosphorus system. Transactions of the American Institute of Mining, Metallurgical and Petroleum Engineers 137, 354–372.

Davis J R (ed), 2001. Copper and copper alloys. Materials Park, OH: ASM International.

Dinsdale A T, 1991. SGTE data for pure elements. Calphad 15, 317–425.

Eichenauer W, Pebler A, 1957. Measurement of the diffusion coefficient and solubility of hydrogen in aluminum and in copper. Zeitschrift für Metallkunde 48, 373–378.

Glaum R, Walter-Peter M, Özalp D, Gruehn R, 1991. Beiträge zum thermischen Verhalten wasserfreier Phospahte. IV. Zum chemischen Transport von Pyrophosphaten $M_2P_2O_7$ (M=Mg, Cr, Mn, Fe, Co, Ni, Cu, Zn, Cd) – Die erstmalige Darstellung von Chrom(II)-pyrophosphat. Zeitschrift für anorganische und allgemeine Chemie 601, 145–162.

Gordienko S P, Viksman G S, 1985. High-temperature behaviur and thermodynamic properties of the compounds Cu_3P and CuP_2. Soviet Powder Metallurgy and Metal Ceramics 7, 573–575.

Grimvall G, 1999. Thermophysical properties of materials. Amsterdam: Elsevier.

Hallstedt B, Gauckler L J, 2003. Revision of the thermodynamic descriptions of the Cu-O, Ag-O, Ag-Cu-O, Bi-Sr-O, Bi-Ca-O, Bi-Cu-O, Sr-Cu-O, Ca-Cu-O and Sr-Ca-Cu-O systems. Computer Coupling of Phase Diagrams and Thermochemistry 27, 177–191.

Hallstedt B, Risold D, Gauckler L J, 1994. Thermodynamic assessment of the copper-oxygen system. Journal of Phase Equilibria 15, 483–499.

Hammer B, Lenz D, Reimers P, Dudzus T, Schmitt B F, 1984. Die Löslichkeit des Sauerstoffs in Reinstkupfer. Metall (Berlin) 38, 41–45.

Hansen M, Anderko K, 1958. Constitution of binary alloys. 2nd ed. New York: McGraw-Hill.

Heyn V E, Bauer O, 1907. Copper and phosphorus. Metallurgie 4, 242–257.

Hillert M, 2001. The compound energy formalism. Journal of Alloys and Compounds 320, 161–176.

Horrigan V M, 1977. The solubility of oxygen in solid copper. Metallurgical Transactions A 8, 785–787.

Huang W, Opalka S M, Wang D, Flanagan T B, 2007. Thermodynamic modelling of the Cu-Pd-H system. Calphad 31, 315–329.

Knacke O, Kubaschewski O, Hesselmann K (eds), 1991. Thermochemical properties of inorganic substances. 2nd ed. Berlin: Springer-Verlag.

Korzhavyi P A, Johansson B, 2010. Thermodynamic properties of copper compounds with oxygen and hydrogen from first principles. SKB TR-10-30, Svensk Kärnbränslehantering AB.

Korzhavyi P A, Soroka I L, Isaev E I, Lilja C, Johansson B, 2012. Exploring monovalent copper compounds with oxygen and hydrogen. Proceedings of the National Academy of Sciences 109, 686–689.

Krull H G, Singh R N, Sommer F, 2000. Generalized association model. Zeitschrift für Metallkunde 91, 356–365.

Kubaschewski O, Alcook C B, 1979. Metallurgical thermochemistry. 5th ed. Oxford: Pergamon.

La Iglesia A, 2009. Estimating the thermodynamic properties of phosphate minerals at high and low temperature from the sum of constituent units. Estudios Geológicos 65, 109–119.

Le S-N, Navrotsky A, Pralong V, 2008. Energetics of copper diphosphates – $Cu_2P_2O_7$ and $Cu_3(P_2O_6OH)_2$. Solid State Sciences 10, 761–767.

Lee B-J, Sundman B, Kim S I, Chin K-G, 2007. Thermodynamic calculations on the stability of Cu_2S in low carbon steels. ISIJ International 47, 163–171.

Lieser K H, Witte H, 1954. Löslichkeit von Wasserstoff in Legierungen IV. Diskussion der Ergebnisse. Zeitschrift für physikalische Chemie 202, 321–351.

Lindlief W E, 1933. Melting points of some binary and ternary copper-rich alloys containing phosphorus. Metals and Alloys 4, 85–88.

Lukas H L, Fries S G, Sundman B, 2007. Computational thermdynamics: the Calphad method. New York: Cambridge University Press.

Lyman T (ed), 1973. Metals handbook. Vol 8. Metallography, structures and phase diagrams. Metals Park, OH: American Society for Metals.

Magalhães M C F, Jesus J P D, 1986. Stability constants and formation of Cu(II) and Zn(II) phosphate minerals in the oxidized zone of base metal orebodies. Mineralogical Magazine 50, 33–39.

Martinsson Å, Sandström R, Lilja C, 2013. Hydrogen in oxygen-free, phosphorus-doped copper: charging techniques, hydrogen contents and modelling of hydrogen diffusion and depth profile. SKB TR-13-09, Svensk Kärnbränslehantering AB.

Massalski T B (ed), 1986. Binary alloy phase diagrams. Vol 1. Metals Park, OH: American Society for Metals.

McLellan R B, 1973. Solid solutions of hydrogen in gold, silver and copper. Journal of Physics and Chemistry of Solids 34, 1137–1141.

Mertz J C, Mathewson C H, 1937. The solid solubilities of the elements of the periodic sub-group Vb in copper. Transactions of the American Institute of Mining, Metallurgical and Petroleum Engineers 124, 59–77.

Miettinen J, 2001. Thermodynamic description of Cu-Sn-P system in the copper-rich corner. Calphad 25, 67–78.

Narula M L, Tare V B, Worrell W L, 1983. Diffusivity and solubility of oxygen in solid copper using potentiostatic and potentiometric techniques. Metallurgical Transactions B 14, 673–677.

Noda T, Oikawa K, Itoh S, Hino M, Nagasaka T, 2009. Thermodynamic evaluation of Cu-Cu_3P system based on newly determined Gibbs energy of formation of Cu_3P. Calphad 33, 557–560.

Okamoto H, 1991. P-S (phosphorus-sulfur). Journal of Phase Equilibria 12, 706–707.

Oudar J, 1959. Solubility of S in Cu at 600–1,000°C. Comptes Rendus 249, 259–261.

Pakarinen J, 2011. (S)TEM analysis of OFP copper CT-tested in S containing groundwater. Research Report VTT-R-04957-11, VTT, Finland.

Puigdomenech I, Taxén C, 2000. Thermodynamic data for copper: Implications for the corrosion of copper under repository conditions. SKB TR-00-13, Svensk Kärnbränslehantering AB.

Röntgen P, Möller F, 1934. The solubility of gases in copper and aluminum. Metallwirtschaft 13, 81–83.

Saunders N, Miodownik A P, 1998. CALPHAD: calculation of phase diagrams: a comprehensive guide. New York: Pergamon.

Savolainen K, 2012. Friction stir welding of copper and microstructure and properties of the welds. PhD thesis. Aalto University, Helsinki, Finland.

Schmid R, 1983. A thermodynamic analysis of the Cu-O system with an associated solution model. Metallurgical Transactions B 14, 473–481.

Schramm L, Behr G, Löser W, Wetzig K, 2005. Thermodynamic reassessment of the Cu-O phase diagram. Journal of Phase Equilibria and Diffusion 26, 605–612.

Shapovalov V I, 1999. Metal-hydrogen phase diagrams in the vicinity of melting temperatures. In Proceedings of AVS International Liquid Metal Processing and Casting Symposium, Santa Fe, NM, 21–24 Februari 1999.

Shishin D, Decterov S A, 2012. Critical assessment and thermodynamic modeling of the Cu-O and Cu-O-S systems. Calphad 38, 59–70.

SKB, 2006. Kapsel för använt kärnbränsle: Tillverkning av kapselkomponenter. SKB R-06-03, Svensk Kärnbränslehantering AB. (In Swedish.)

SKB, 2009. Design premises for a KBS-3V repository based on results from the safety assessment SR-Can and some subsequent analyses. SKB TR-09-22, Svensk Kärnbränslehantering AB.

SKB, 2010. Design, production and initial state of the canister. SKB TR-10-14, Svensk Kärnbränslehantering AB.

Smart J S, Smith A A, 1946. Effect of phosphorus, arsenic, sulphur, and selenium on some properties of high-purity copper. Transactions of the American Institute of Mining, Metallurgical and Petroleum Engineers 166, 144–155.

Subramanian P R, Laughlin D E, 1994. Cu-P. In Subramanian P R, Chakrabarti D J, Laughlin D E (eds). Phase diagrams of binary alloys. Materials Park, Ohio: ASM International, 295–300.

Sundman B, Ågren J, 1981. A regular solution model for phases with several components and sublattices, suitable for computer applications. Journal of Physics and Chemistry of Solids 42, 297–301.

Sverchkova A K, Andreev L A, Minaev Y A, 1989. Effect of crystal structure on the solubility of hydrogen in copper. Metal Science and Heat Treatment 31, 833–836.

Tanabe T, Yamanishi Y, Sawada K, Imoto S, 1984. Hydrogen transport in stainless steels. Journal of Nuclear Materials 123, 1568–1572.

Thermo-Calc, 2010. Thermo-Calc software, version S (build 2532). Stockholm: Thermo-Calc Software AB.

Thomas C L, 1967. Solubility of hydrogen in solid copper, silver, and gold obtained by a rapid quench and extraction technique. Transactions of the American Institute of Mining, Metallurgical and Petroleum Engineers 239, 485–496.

Vieillard P, Tardy Y, 1984. Thermochemical properties of phosphates. In Nriagu O, Moore P B (eds). Phosphate minerals. Berlin: Springer, 171–198.

Wagman D D (ed), 1982. The NBS tables of chemical thermodynamic properties: selected values for inorganic and C_1 and C_2 organic substances in SI units. New York: American Chemical Society.

Zhang Q-X, Smeltzer W W, Jinshu Y, 1987. Diffusivity and solubility of oxygen in crystal solid copper. Chinese Non-Ferrous Metals 39, 57–61.

Appendix 1

Parameters in thermodynamic model

A1.1 Standard element reference and thermochemical quantities

Gibbs energy for each phase is given relative the standard element reference, which in this work is defined as the enthalpy of the pure element in its reference phase at 298.15 K (Dinsdale 1991). The reference phase is chosen as the stable phase at 298.15 K and 100 kPa, except phosphorus for which the white phase is taken. The reference phase and the corresponding Gibbs energy at 298.15 K is given in Table A1-1. As a consequence, other tabulated data such as the work by Puigdomenech and Taxén (2000) uses the reference for copper ${}^{\circ}G_{Cu}^{FCC}(298.15) = 0$. In this work, ${}^{\circ}H^{REF}(298.15) = 0$ that results in ${}^{\circ}G_{Cu}^{FCC}(298.15) = -298.15 \cdot {}^{\circ}S_{Cu}^{FCC} = -9.884$ kJ per mole. The formation energies for pure compounds and elements are therefore lower than previous work. On the other hand, quantities that have a defined absolute value, such as heat capactiy and entropy, are identical. In addition, a relative value in Gibbs energy like the formation energy from the elements will also be identical as long as the element contributions are included.

Table A1-1. Element and their reference phase and Gibbs energy at 298.15 K and 100 kPa given in J per atom mole.

Element	Phase	G(298.15) J / atom mol
Cu	FCC	–9,883.672
½H_2	Gas	–19,464.806
½O_2	Gas	–30,548.980
S	Orthorhombic	–9,556.901
P	White	–12,247.106

The following relations can be used to evaluate enthalpy H, entropy S or heat capacity C_p from Gibbs energy expressions G:

$$G = a + bT + cTlnT + dT^2 + eT^{-1} + fT^3 \quad \text{(A1-1)}$$

$$S = -\frac{dG}{dT} = -(b + c) - clnT - 2dT + eT^{-2} - 3fT^2 \quad \text{(A1-2)}$$

$$H = G - T\frac{dG}{dT} = a - cT - dT^2 + 2eT^{-1} - 2fT^3 \quad \text{(A1-3)}$$

$$C_p = \frac{dH}{dT} = -T\frac{d^2G}{dT^2} = -c - 2dT - 2eT^{-2} - 6fT^2 \quad \text{(A1-4)}$$

A1-2 Assessed parameters

All evaluated parameters for liquid and FCC phase is given in Table A1-2 for the binary systems including copper for the Cu-H-O-S-P system. In this table, gas phase is included for oxygen and hydrogen since this is the reference phase for these elements. In similarity, the sulphur orthorhombic and phosphorus white phases are included as well. Evaluated coefficients of Gibbs energy expressions for stoichiometric phases are given in Table A1-3. Stability of all species in the gas phase is given in Table A1-4.

Table A1-2. Thermodynamic parameters of all binary systems including Cu for the Cu-H-O-S-P system. Complete set of parameters are included for FCC and liquid phases. Other phases are given only if reference phases for elements. (*) is evaluated in this work.

Phase, constituents, and model parameters	Ref.
Gas (H_2,O_2,…), element reference hydrogen and oxygen	
${}^{\circ}G_{O_2}^{gas} = +RTlnP + 2 \cdot$ $(T < 1000): -3480.87 - 25.5031T - 11.1355TlnT - 5.09888 \cdot 10^{-3}T^2 + 0.66184 \cdot 10^{-6}T^3 - 38365T^{-1}$ $(1000 < T < 3300): -6568.76 + 12.65988T - 16.8138TlnT - 5.9579 \cdot 10^{-4}T^2 + 0.006781 \cdot 10^{-6}T^3 + 262905T^{-1}$ $(3300 < T < 6000): -13986.73 + 31.259T - 18.9536TlnT - 4.2524 \cdot 10^{-4}T^2 + 0.0107 \cdot 10^{-6}T^3 + 4383200T^{-1}$	(1)
${}^{\circ}G_{H_2}^{gas} = +RTlnP +$ $(T < 1000): -9522.9739 + 78.5274T - 31.3571TlnT + 0.00275899T^2 - 7.46391 \cdot 10^{-7}T^3 + 56582.3T^{-1}$ $(1000 < T < 2100): +180.1088 - 15.61283T - 17.8486TlnT - 0.005842T^2 + 3.1462 \cdot 10^{-7}T^3 - 1280036T^{-1}$ $(2100 < T < 6000): -18840.16 + 92.312T - 32.0508TlnT - 0.001073T^2 + 1.1428 \cdot 10^{-8}T^3 + 3561002.5T^{-1}$	(1)
Other gas species beside H_2 and O_2 evaluated in this work, see Table A1-4.	
O, PO, SO, S_2O, PO_2, SO_2, O_3, SO_3, P_4O_6, P_4O_{10}, H, OH, HO_2, PH, SH, H_2O, H_2O_2, H_2SO_4, PH_2, H_2S, PH_3, P, PS, P_2, P_4, P_4S_3, S_1, S_2, S_3, S_4, S_5, S_6, S_7, S_8, Cu, CuO, Cu_2	*
Liquid (Cu,H,O,S,P,Cu_2O,Cu_2S)	
${}^{\circ}G_{Cu}^{liquid} =$ $(T < 1357.77): {}^{\circ}G_{Cu}^{fcc} + 12964.735 - 9.511904T - 584.89 \cdot 10^{-23}T^7$ $(T > 1357.77): -46.545 + 173.881484T - 31.38TlnT$	(1)
${}^{\circ}G_{P}^{liquid} =$ $(T < 317.3): -26316.1 + 434.943931T - 70.744058TlnT - 0.00289894T^2 + 3.904934 \cdot 10^{-5}T^3 + 1141147T^{-1}$ $(T > 317.3): -7232.449 + 133.30487T - 26.326TlnT$	(1)
${}^{\circ}G_{S}^{liquid} =$ $(T < 388.36): -4001.55 + 77.9057T - 15.504TlnT - 0.01863T^2 - 2.494 \cdot 10^{-7}T^3 - 113945T^{-1}$ $(388.36 < T < 428.15): -5285183.35 + 118449.601T - 19762.4TlnT + 32.79275T^2 - 0.0102214T^3 + 2.646735 \cdot 10^{8}T^{-1}$ $(428.15 < T < 432.25): -8174995.2 + 319914.0T - 57607.3TlnT + 135.3045T^2 - 0.052997T^3$ $(432.25 < T < 453.15): -219408.801 + 7758.856 - 1371.85TlnT + 2.845T^2 - 0.001014T^3$ $(453.15 < T < 717): +92539.87 - 1336.35T + 202.958TlnT + 5.1884 \cdot 10^{-5}T^3 - 8202200T^{-1}$ $(717 < T): -6889.972 + 176.3708T - 32TlnT$	(1)
${}^{\circ}G_{O}^{liquid} - {}^{\circ}G_{0.5O_2}^{gas} = -2648.9 + 31.44T$	(1)
${}^{\circ}G_{H}^{liquid} - {}^{\circ}G_{0.5H_2}^{gas} = +8035 + 25T + 2TlnT$	(2)
${}^{\circ}G_{Cu_2O}^{liquid} - 2{}^{\circ}G_{Cu}^{fcc} - {}^{\circ}G_{0.5O_2}^{gas} = -119801 + 90.34T - 6.79TlnT$	(3)
${}^{\circ}G_{Cu_2S}^{liquid} - {}^{\circ}G_{Cu_2S}^{dig} = +22136 - 15.6267T$	(4)
${}^{0}L_{Cu,H}^{liquid} = +45068 - 11T$	*
${}^{0}L_{Cu,P}^{liquid} = -180379 + 101.068T$	(5)
${}^{1}L_{Cu,P}^{liquid} = +39496 - 91.505T$	(5)
${}^{3}L_{Cu,P}^{liquid} = +35583$	(5)
${}^{0}L_{Cu,Cu_2O}^{liquid} = +63686 - 19.9T$	*
${}^{1}L_{Cu,Cu_2O}^{liquid} = +14100 - 9.3T$	*
${}^{0}L_{Cu,Cu_2S}^{liquid} = +85840 - 27.6287T$	(4)
${}^{1}L_{Cu,Cu_2S}^{liquid} = -12900 + 8.5262T$	(3)
${}^{0}L_{Cu_2S,S}^{liquid} = +40406.6 - 17.5576T$	(3)
${}^{1}L_{Cu_2S,S}^{liquid} = -100287 + 35.0356T$	(3)

Phase, constituents, and model parameters	Ref.
FCC (Cu,S,P)$_1$(H,O,Va)$_1$	
${}^{\circ}G^{fcc}_{Cu:Va}=$	(1)
$(T < 1357.77)$: $-7770.458 + 130.485235T - 24.112392TlnT - 2.65684 \cdot 10^{-3}T^2 + 0.129223 \cdot 10^{-6}T^3 + 52478T^{-1}$	
$(T > 1357.77)$: $-13542.026 + 183.803828T - 31.38TlnT + 364.167 \cdot 10^{27}T^{-9}$	
${}^{\circ}G^{fcc}_{P:Va}=$	(1)
$(T < 500)$: $10842.441 + 135.534T - 25.55TlnT + 3.4121 \cdot 10^{-3}T^2 - 2.41887 \cdot 10^{-6}T^3 + 160095T^{-1}$	
$(500 < T < 852.35)$: $15095.279 + 64.533737T - 14.368TlnT - 9.57685 \cdot 10^{-3}T^2 + 0.39391 \cdot 10^{-6}T^3 - 141375T^{-1}$	
$(852.35 < T < 1500)$: $-82589.413 + 1012.8916T - 149.44956TlnT + 67.2724 \cdot 10^{-3}T^2 - 6.65193 \cdot 10^{-6}T^3 + 12495943T^{-1}$	
$(1500 < T)$: $+12294.881 + 140.70118T - 26.326TlnT$	
${}^{\circ}G^{fcc}_{S:Va} - {}^{\circ}G^{ortho}_{S} = 105000$	(4)
${}^{\circ}G^{fcc}_{Cu:H} - {}^{\circ}G^{fcc}_{Cu} - {}^{\circ}G^{gas}_{0.5H_2} = 60880 + 36.9T$	*
${}^{\circ}G^{fcc}_{Cu:O} - {}^{\circ}G^{fcc}_{Cu} - {}^{\circ}G^{gas}_{0.5O_2} = -19400 + 31T$	(6)
${}^{0}L^{fcc}_{Cu,P:Va} = -109505 + 14.434T$	(5)
${}^{0}L^{fcc}_{Cu:H,Va} = -5377$	*
${}^{0}L^{fcc}_{Cu,S:Va} = -102200 - 26.5T$	(4)
White (P), element reference phosphorus	
${}^{\circ}G^{white}_{P} =$	(1)
$(T < 317.3)$: $-43821.799 + 1026.7069T - 178.426TlnT + 0.29071T^2 - 1.04023 \cdot 10^{-4}T^3 + 1632695T^{-1}$	
$(317.3 < T < 1000)$: $-9587.5 + 152.35T - 28.7335TlnT + 0.001716T^2 - 2.2829 \cdot 10^{-7}T^3 + 172966T^{-1}$	
$(1000 < T)$: $-8093.075 + 135.8898T - 26.326TlnT$	
Orthorhombic (S), element reference sulfur	
${}^{\circ}G^{ortho}_{S} =$	(1)
$(T < 368.3)$: $-5228.956 + 55.4178T - 11.007TlnT - 0.02653T^2 + 7.7543 \cdot 10^{-6}T^3$	
$(368.3 < T)$: $-6513.769 + 94.6929T - 17.942TlnT - 0.010895T^2 + 1.40256 \cdot 10^{-6}T^3 + 39910T^{-1}$	
CuH_wurtzite	
${}^{\circ}G^{CuH}_{Cu:H} - {}^{\circ}G^{fcc}_{Cu} - {}^{\circ}G^{gas}_{0.5H_2} = 36700 + 47.62T$	(7)
CuH_sphalerite	
${}^{\circ}G^{CuH}_{Cu:H} - {}^{\circ}G^{fcc}_{Cu} - {}^{\circ}G^{gas}_{0.5H_2} = 37950 + 47.62T$	(7)
Water, H_2O	
${}^{\circ}G^{Water}_{H_2O} =$	*
$(T < 428.02)$: $-429699 + 3315.01T - 561.063TlnT + 0.85897T^2 + 5.64359 \cdot 10^{6}T^{-1} - 0.000284616T^3$	
$(428.02 < T < 647)$: $-357088 + 1733.19T - 287.921TlnT + 0.241782T^2$	
Other phases evaluated in this work, see Table A1-3	
CuOH, Cu_2SO_4, $CuSO_4$, $CuO{\cdot}CuSO_4$, CuO, CuH_2O_2, $Cu_2P_2O_7$, $Cu_3P_2O_8$, P_4S_5, P_4S_7, P_2S_5, P_4S_3, P_4O_{10}, Poitevinite ($CuSO_4{\cdot}1H_2O$), Bonattite ($CuSO_4{\cdot}3H_2O$), Chalcanthite ($CuSO_4{\cdot}5H_2O$), Langite ($CuSO_4{\cdot}3Cu(OH)_2{\cdot}H_2O$), Antlerite ($CuSO_4{\cdot}2Cu(OH)_2$), Brochantite ($CuSO_4{\cdot}3Cu(OH)_2$), Libethenite ($Cu_2PO_4(OH)$), Cornetite ($Cu_3PO_4(OH)_3$), Pseudomalachite ($Cu_5(PO_4)_2(OH)_4$), $Cu_3(PO_4)_2{\cdot}2H_2O$, $Cu_3(PO_4)_2{\cdot}3H_2O$, $Cu_3(P_2O_6OH)_2$	*
Other phases, given with reference	
Cu_3P	(5)
Cu_2O	(6)
Digenite (Cu_2S), *α*-Chalcocite (Cu_2S), β-Chalcocite (Cu_2S), Anilite ($Cu_{1.75}S$), Djurleite ($Cu_{1.93}S$), and Covellite (CuS)	(4)
Monoclinic (S), and Red (P)	(1)
References	
(1) Dinsdale 1991, (2) Huang et al. 2007, (3) Clavaguera-Mora et al. 2004, (4) Lee et al. 2007, (5) Noda et al. 2009, (6) Hallstedt and Gauckler 2003 , (7) Korzhavyi and Johansson 2010	

Table A1-3. Coefficients in Gibbs energy expressions for all stable crystalline phases. Phases denoted with † uses other expressions according to their evaluations, but have been summarised in this table on the same form for comparison.

Compound	a	b	c	d	e
CuP_2	–141,011	354.237	–64.087	–0.01130	–16,474.8
Cu_3P †	–134,190	517.681	–95.475	–0.008689	–71,271.9
Cu_2S *Digenite* †	–102,093	342.949	–70.852	–0.005177	661,512
Cu_2S *α-Chalcocite* †	–106,716	356.917	–71.762	–0.005177	661,512
Cu_2S *β-Chalcocite* †	–108,000	384.339	–75.963	–0.005177	661,512
$Cu_{1.75}S$ *Anilite* †	–102,212	384.053	–72.794	–0.004705	641,681
$Cu_{1.93}S$ *Djurleite* †	–107,392	400.289	–77.279	–0.005045	655,959
CuS *Covellite* †	–72,924.5	298.399	–54.104	–0.003290	582,190
Cu_2O †	–193,230	360.057	–66.260	–0.007960	374,000
CuO	–173,000	289.350	–48.592	–0.003720	381,000
P_4S_5	–362,169	955.611	–175.017	–0.06019	0
P_4S_7	–387,038	1,001.82	–187.264	–0.09196	0
P_2S_5	–223,859	561.353	–106.047	–0.07008	0
P_4S_3	–250,568	63.2481	–18.2415	–0.24186	0
CuH_wurtzite†	25,275.4	202.782	–37.6066	–0.00303	–15,515.8
CuH_sphalerite†	26,525.4	202.782	–37.6066	–0.00303	–15,515.8
CuH_halite†	49,455.4	192.062	–37.6066	–0.00303	–15,515.8
CuOH	–214,259	299.536	–45.8266	–0.00334	74,483.5
$Cu(OH)_2$	$-4.73\cdot10^5$	557.73	–97.753	–0.010958	$4.31\cdot10^5$
P_4O_{10}	$-3.08\cdot10^6$	893.70	–150.54	–0.161870	$1.57\cdot10^6$
$Cu_2P_2O_7$	$-2.15\cdot10^6$	927.22	–172.45	–0.08838	$1.55\cdot10^6$
$Cu_3(PO_4)_2$	$-2.34\cdot10^6$	1,187.1	–221.05	–0.092095	$1.93\cdot10^6$
Cu_2SO_4	$-7.84\cdot10^5$	505.24	–99.578	–0.03473	–34.024
$CuSO_4$	$-8.23\cdot10^5$	782.15	–128.91	–0.01395	$1.75\cdot10^6$
$CuO\cdot CuSO_4$	$-9.90\cdot10^5$	1,009	–170.83	–0.02268	$1.96\cdot10^6$
$Cu_2PO_4(OH)$, *Libethenite*	$-1.42\cdot10^6$	872.41	–159.40	–0.05153	$1.18\cdot10^6$
$Cu_3PO_4(OH)_3$, *Cornetite*	$-1.90\cdot10^6$	1,430.1	–257.15	–0.06248	$1.61\cdot10^6$
$Cu_5(PO_4)_2(OH)_4$, *Pseudomalachite*	$-3.34\cdot10^6$	2,302.6	–416.56	–0.11401	$2.79\cdot10^6$
$Cu_3(PO_4)_2\cdot2H_2O$	$-2.98\cdot10^6$	1,508.3	–277.86	–0.10457	$1.80\cdot10^6$
$Cu_3(PO_4)_2\cdot3H_2O$	$-3.24\cdot10^6$	1,632.9	–306.27	–0.11081	$1.74\cdot10^6$
$Cu_3(P_2O_6OH)_2$	$-4.43\cdot10^6$	1,756.2	–324.73	–0.17927	$2.65\cdot10^6$
$CuSO_4\cdot1H_2O$, *Poitevinite*	$-1.13\cdot10^6$	762.49	–130.79	–0.0354	930,940
$CuSO_4\cdot3H_2O$, *Bonattite*	$-1.75\cdot10^6$	1,177.9	–204.31	–0.0359	920,480
$CuSO_4\cdot5H_2O$, *Chalcanthite*	$-2.37\cdot10^6$	1,612.1	–280.96	–0.0354	928,848
$CuSO_4\cdot3Cu(OH)_2\cdot H_2O$, *Langite*	$-2.63\cdot10^6$	2,570.9	–424.05	–0.0683	$2.22\cdot10^6$
$CuSO_4\cdot2Cu(OH)_2$, *Antlerite*	$-1.85\cdot10^6$	1,957.2	–324.42	–0.0359	$2.61\cdot10^6$
$CuSO_4\cdot3Cu(OH)_2$, *Brochantite*	$-2.34\cdot10^6$	2,550.0	–422.17	–0.0468	$3.04\cdot10^6$

Table A1-4. Coefficients in Gibbs energy expressions for all gas species. Experimental data is mainly taken from NIST-JANAF (Chase 1998) and NBS tables (Wagman 1982). Gases H_2 and O_2 are given in Table A1-2. Thermochemical data is evaluated for temperatures 298–2,000 K.

Compound	a	b	c	d	e	f
O	243,213	–20.906	–21.010	0.000128	–43,627.5	$-1.30\cdot10^{-8}$
PO	–31,749.6	–21.067	–30.469	–0.00378	42,844.5	$3.48\cdot10^{-7}$
SO	–5,574.92	–7.723	–31.501	–0.00294	141,623	$1.92\cdot10^{-7}$
S_2O	–83,731.1	72.282	–49.641	–0.00464	371,575	$4.48\cdot10^{-7}$
PO_2	–332,146	73.795	–47.672	–0.00576	435,760	$5.60\cdot10^{-7}$
SO_2	–312,343	42.097	–42.034	–0.00884	331,100	$8.09\cdot10^{-7}$
O_3	125,664	70.387	–44.781	–0.00756	451,113	$7.05\cdot10^{-7}$
SO_3	–418,497	143.508	–57.497	–0.01352	663,827	$1.28\cdot10^{-6}$
P_4O_6	$-1.80\cdot10^{6}$	1,019.83	–197.295	–0.01973	$2.92\cdot10^{6}$	$1.93\cdot10^{-6}$
P_4O_{10}	$-3.05\cdot10^{6}$	1,330.65	–248.61	–0.04524	$3.88\cdot10^{6}$	$4.35\cdot10^{-6}$
H	211,802	24.500	–20.786	0	0	0
OH	31,753.8	–8.132	–26.213	–0.00222	–116,146	$1.32\cdot10^{-8}$
HO_2	–9,331.73	–4.970	–32.396	–0.00965	140,588	$6.61\cdot10^{-7}$
PH	226,514	–32.117	–24.201	–0.00538	–86,841.8	$3.50\cdot10^{-7}$
SH	127,780	–21.497	–25.99	–0.00392	–197,066	$2.28\cdot10^{-7}$
H_2O	–249,362	–13.684	–25.575	–0.00913	–130,617	$4.53\cdot10^{-7}$
H_2O_2	–153,084	77.355	–44.591	–0.01276	388,645	$1.06\cdot10^{-6}$
H_2SO_4	–774,277	375.639	–96.462	–0.02533	$1.23\cdot10^{6}$	$2.07\cdot10^{-6}$
PH_2	99,709.8	–28.807	–26.329	–0.01372	–33,435.1	$1.13\cdot10^{-6}$
H_2S	–28,240.5	–36.017	–24.343	–0.0136	–101,239	$1.01\cdot10^{-6}$
PH_3	–11,688.8	–20.813	–25.834	–0.02568	149,176	$2.18\cdot10^{-6}$
P	310,034	–21.376	–21.191	0.000397	9,912.43	$-6.39\cdot10^{-8}$
PS	127,137	11.799	–36.555	–0.00062	75,434.8	$4.67\cdot10^{-8}$
P_2	131,975	18.406	–34.902	–0.00152	169,460	$1.38\cdot10^{-7}$
P_4	30,658.4	264.791	–80.145	–0.00171	625,747	$1.70\cdot10^{-7}$
P_4S_3	–197,226	717.577	–154.808	0	0	0
S_1	270,276	–9.633	–23.833	0.001753	–38,708.7	$-1.87\cdot10^{-7}$
S_2	37,466.6	8.319	–34.945	–0.00133	146,123	$-3.12\cdot10^{-11}$
S_3	123,034	95.666	–53.7822	–0.00217	325,130	$-1.08\cdot10^{-10}$
S_4	117,741	233.058	–80.0312	–0.00157	595,980	$-5.02\cdot10^{-9}$
S_5	72,115.7	416.801	–106.935	–0.00053	788,920	$-7.49\cdot10^{-11}$
S_6	56,311.6	541.368	–132.131	–0.00025	920,508	$-5.64\cdot10^{-11}$
S_7	60,712.4	642.089	–154.967	–0.00128	988,055	$-8.67\cdot10^{-11}$
S_8	36,522.5	782.491	–179.069	–0.0022	$1.09\cdot10^{6}$	$2.20\cdot10^{-7}$
Cu	331,162	–23.077	–21.424	0.000625	15,622.3	$-1.00\cdot10^{-7}$
CuO	294,785	13.284	–36.850	–0.00058	67,369.8	$2.96\cdot10^{-8}$
Cu_2	473,879	9.216	–37.356	–0.0004	44,870.9	$3.27\cdot10^{-9}$